WOLLEGA UNIVERSITY

SCHOOL OF GRADUATE STUDIES

STRUCTURAL AND COMPLEX IMPEDANCE PROPERTY STUDY OF LEAD TITANATE (PT) CERAMIC MATERIAL: A REVIEW RESEARCH

MSc Thesis

By

DEREJE BIYENA

JUNE, 2021

NEKEMTE, ETHIOPIA

WOLLEGA UNIVERSITY

SCHOOL OF GRADUATE STUDIES

Structural and complex impedance property study of lead titanate (PT) ceramic material: A research Review

A thesis submitted to school of graduate studies in partial fulfillment of the requirements for degree of master of physics (Condensed matter physics)

By

Dereje Biyena

Advisor: Dr. Kebede Legesse Kebeta

April, 2021

Nekemte, Ethiopia

STATEMENT OF THE AUTHOR

I declare that this Thesis entitled Structural and complex impedance property study of lead titanate (PT) ceramic material ″ is my work and that all sources of materials used for this thesis have been appropriately acknowledged.

This thesis is submitted in partial fulfillment of the requirements for Msc degree in physics at Wollega University. I seriously declare that this thesis is not submitted to any other institution anywhere for the award of any degree or diploma. The thesis deposited at the university library to make available to borrowers under rules of the wollega university library. Brief quotations from this thesis are allowable without special permission if accurate acknowledgment of the source is made. However, requests for permission for extended quotations from or reproduction in part of this manuscript may be granted by Wollega University, the school of graduate studies in all other instances, permission must be obtained from the author.

Name: _____Signature: _____ Date _____

Place: Wollega University, Nekemte

DECLARATION

This is to certify that this thesis entitled “Structural and complex impedance property study of lead titanate (PT) ceramic material” accepted in partial fulfillment of the requirements for the award of the degree of MSc in Physics by the school of Graduate Studies, Wollega University through the college of Natural and computational science done by Dereje Biyena is a genuine work carried out by him under my guidance. The matter embodied in this thesis work has not been submitted earlier for the award of any degree or diploma. The assistance and help received during the course of this investigation have been duly acknowledged. Therefore, I recommend that it can be accepted as fulfilling the research thesis requirements.

_____	_____	_____
Advisor	Signature	Date

WOLLEGA UNIVERSITY

SCHOOL OF GRADUATE STUDIES

FINAL THESIS APPROVAL FORM

As members of the board of examining of the final M.sc thesis open defense, we certify that we have read and evaluated the thesis prepared by Dereje Biyena under the title ″ Structural and complex impedance property study of lead titanate (PT) ceramic material″& recommend that the thesis can be accepted as fulfilling the thesis requirement for the degree of masters in physics.

Chairperson	Signature	Date
Internal Examiner	Signature	Date
External Examiner	Signature	Date

Final Approval and Acceptance

Thesis Approved by

Department PGC	Signature	Date
Dean of SGS	Signature	Date

CERTIFICATION OF THE FINAL THESIS

I hereby certify that all the correction and recommendation suggested by the board of the examiners are incorporated in to final thesis ″ the Structural and complex impedance property study of lead titanate (PT) ceramic material by Dereje Biyena.

Dean of SGS	Signature	Date

ACKNOWLEDGEMENT

First of all, I would like to praise the almighty God for my successes who initiated to begin and enable to accomplish everything. Next, I would like to thank my special appreciation & heart felt gratitude goes to my advisor Dr. Kebede Legesse for his guidance & much needed support, friendly treatment, critical remark & encouragement through out my study periods. I would like to express my deepest gratitude to him for his encourage & positive approach.

ABBREVIATIONS AND ACRONYMS

ABO_3: perovskite structure formula

BT: Barium titanate

CMOS: Complementary metal oxide semiconductor

CSD: Chemical solution deposition

FE: Ferroelectric

FeRAM: Ferroelectric random access memory

MEMS: Microelectromechanical system

MgO: Magnesium Oxide

MOCVD: Metal organic vapor deposition

Nb_2O_5: Niobium pentoxide

PbO: Lead monoxide

PMN: Lead magnesium niobate

PT: Lead titanate

PZT: Lead zirconate titanate

RFE**:** Relaxor ferroelectric

RT: Room temperature

SSR: Solid state reaction

XRD: X-ray Diffraction

CONTENTS

LIST OF TABLES

LIST OF FIGURES

ABSTRACT

The semiconductor industry is one of the most developed and expanding branches in the world. Crystals of the perovskitefamily, such as PbTiO3, BaTiO3, SrTiO3 and, have been of constant interest because some of these materials show ferroelectric behavior and undergo structural phase transitions [ZVEI, March 2005]. PbTiO3 has been considered to be one of the most important members of this family. The objective of this study was Structural and complex impedance property study of lead titanate (PT) ceramic material. Single-phase polycrystalline samples of lead titanate with perovskite structure have been synthesized using solid-state reaction technique. Lead titanate thin films were also prepared by the sol synthesis from acetylacetone/ethylene glycol route by a sol–gel method. The thin films were deposited by a spin coating technique by utilizing the as-prepared PT-sol (precoating 1,000 rpm for 10 s. followed by 4,000 rpm for 30s.) The influence of film thickness, pyrolysis temperature, and heating rate on (the formation of thin films) microstructure and morphology of thin films have been systematically investigated. The processing parameters have been optimized to obtain phase pure, dense, crack-free, and homogeneous samples. The sintering behavior of PT-powders has been investigated using X-ray diffraction patterns. The X-ray powder diffraction data have been analyzed to confirm the phase formation and phase purity, to obtain unit cell parameters and unit cell volume. The porosity of the samples has been obtained through X-ray density and bulk density. The average particle sizes of the phase pure samples were obtained from the X-ray peak width using Scherrer's formula. The influence of sintering temperature and time on the microstructure of samples has also been studied by carrying out SEM investigations. The notable feature of this microstructure study shows that the samples sintered at 900°C for 12 hours possess a fairly uniform grain distribution. The electrical behavior (complex impedance Z^*, complex permittivity *, etc.) of the samples sintered at 900°C for 12 hours has been studied by complex impedance spectroscopy. The temperature variation of real permittivity gives evidence of the ferroelectric phase transition as well as of the relaxation behavior.

Keywords: **PT; X-ray; SEM; short circuit current;**

CHAPTER 1: INTRODUCTION

1.1. Back ground and Justification

The semiconductor industry is one of the most developed and expanding branches in the world. Crystals of the perovskitefamily, such as PbTiO3, BaTiO3, SrTiO3 and, have been of constant interest because some of these materials show ferroelectric behavior and undergo structural phase transitions (ZVEI, March 2005). PbTiO3 has been considered to be one of the most important members of this family. It has a high Curie temperature, high pyroelectric coefficient, low dielectric constant, and high spontaneous polarization (Y. Matsuo,). Lead titanate (PbTiO3, PT) is a ferroelectric ceramic that has not been proved to be a technologically important material by itself but is a significant component material in electronics such as capacitors, ultrasonic transducers, thermistors, and optoelectronics (S. Jeong, et al.,). It is also a promising material for pyroelectric infrared detector applications because of its large pyroelectric coefficient and relatively low permittivity (H. Yasui, A., Seifert, et al.,). PbTiO3 (PT) has also been extensively used in a range of piezoelectric applications, as well as being the end member of technologically significant ferroelectric perovskite series such as $PbZr_{(x)}Ti(1-x)O_3$(PZT),$Pb_{(x)}Ca(1-x)TiO3$,$Pb(Zn_{1/3}\ Nb_{2/3})O3$-(x) PbTiO3 (PZN-PT), and $Pb(Mg_{1/3}Nb_{2/3})O3$-(x) PbTiO3(PMN-PT)and so forth. At ambient temperature, the material has a strong anisotropy which develops during cooling through the cubic-tetragonal phase transition of approximately 490°C. The anisotropy as measured by the tetragonality of the unit cell, c/a, may be as high as~1.06. A large c/a ratio is considered favorable for enhanced electrical properties (R. Maas, P. Verardi, et al.).

1.2. Statement of the problem

Applications of ferroelectric materials in modern microelectronics will be greatly encouraged if the thermal incompatibility between inorganic ferroelectrics and semiconductor devices is overcome. Here, solution processable layers of the most commercial ferroelectric compound morphotrophic phase boundary lead zirconate titanate, namely $Pb(Zr_{0.52}Ti_{0.48})O_3$ (PZT) are grown on silicon substrates at temperatures well below the standard CMOS process of semiconductor technology.

Hence, the researchers were interested to study the current development in lead titanate(PT) which is one of the ferroelectric materials in modern microelectronics and the gap was filled on the

issue. The main reason of choosing the PT is it is one of the most widely used and investigated ferroelectric material.

1.3. Objective of the study

1.3.1 General objectives

The general objective of the study was to to study structural and complex impedance property study of lead titanate (PT) ceramic material.

1.3.2. Specific objectives

- To resolve definitional ambiguities and outline the scope of the topic
- To provide an integrated, synthesized overview of the current state of knowledge.
- Evaluate existing methodological approaches and unique insights.
- Describe research insights, existing gaps, and future research directions.

1.4. Significance of the Study

Ferroelectric oxides are materials of high interest in electronics owing to their inherent multi-functionality in advanced devices making use of their ferro-, pyro-, piezo- and optoelectronic properties.Relaxors are used as capacitors due to their high permittivity, they used as non-volatile memories and used as sensors and actuators due to their high piezoelectric effects.

1.5. Thesis Organization

This thesis is organized to the following chapter. Chapter 1 is the preliminaries of the Research, introduction, objectives of the study, statement of the problem, and significance of the study. Chapter 2 provides theory and literature review. Chapter 3 focuses on materials and methods. Chapters 4 Result and discussion. Chapters 5 contain conclusion and recommendations.

CHAPTER 2: THEORY OF THE STUDY

Ferroelectric oxides are materials of high interest in electronics owing to their inherent multifunctionality in advanced devices making use of their ferro-, pyro-, piezo- and optoelectronic properties (International jour. 2019). The major obstacle for the integration of these active layers with CMOS (complementary metal-oxide semiconductor) circuits lies on the high processing temperatures required for the crystallization of the ferroelectric oxide, over 600°C. The thermal budget currently recommended for manufacturing sub-100 nm semiconductor devices sets a maximum limit of temperature of 450°C (F. Jona and G. Shirane,). Higher thermal loads may produce excessive dopant diffusion from the source/drain, leading to a short-channel effect that degrades transistor performance and manufacturability. In addition, ferroelectric oxide thin films (mainly lead-based and bismuth-layered perovskite compositions) are considered a potential extra-source of pollution due to the volatilization of high-vapor pressure elements such as Pb and Bi at the temperatures required for the film fabrication (K. Sasazawa,). Metal contamination is a well-known problem in the standard CMOS process that results in circuitry degradation and cross-contamination of back end of the line equipment. Besides the technological issue, the release of hazardous lead towards the atmosphere is also a global subject of environmental concern (T. R. Shrout and A. Halliyal), being of high interest the development of new processing technologies that avoid the emission of toxic volatiles. Therefore, the reduction of the annealing temperature of ferroelectric oxide films is still a key challenge for their full integration into Si-based semiconductor chips.

Although significant efforts have been devoted to the low-temperature processing of ferroelectric oxide thin films using different techniques, the limited success obtained at the moment (UV-assisted annealing (T. R. Shrout and A. Halliyal), laser annealing process (L. E. Cross,), microwave irradiation (L. E. Cross,), seeding approach (D. Damjanovic,), process engineering (L. E. Cross,) or most recent heterogeneous photo catalysis reveals the big complexity of this task. Special attention has been paid to chemical solution deposition (CSD) methods since among other benefits such as comparatively low cost, compositional control and high-throughput fabrication – they offer the particular advantage of tailoring the solution chemistry to attain a low-temperature fabrication of these materials (D. Damjanovic,). Although coating of 3D structures can also be obtained from liquid precursors by mist deposition (Chen G, Zhang), most

electronic devices with commercial success fabricated by CSD (Chen G, Zhang), display a planar ferroelectric-capacitor configuration that finds important applications in multiple fields as sensors (e.g., infrared detectors), transducers (e.g., fingerprint scanners), actuators (e.g., ultrasonic micromotors), or non-volatile memories (e.g., smart cards). The latest ITRS report (Butler KT, Frost JM and Walsh A (2014)) predicts the use of 1T1C (one-transistor, one-capacitor) stack cells in FeRAM (ferroelectric random access memory) technology up to 2028, a device structure where CSD may play an important role for low memory density products.

The road to the thermal compatibility between inorganic ferroelectrics and the standard CMOS process of semiconductors is however not straightforward. The decrease of the annealing temperature of the oxide layers results in incipient crystallization of the required crystalline phases (besides stabilization of detrimental secondary phases) and limited densification of the film, risking poor electrical and mechanical performance. These handicaps are today circumvented only by a few approaches, most of them entailing technical drawbacks for a potential integration into CMOS devices. For instance, laser lift-off techniques without any growth temperature limitation are successful in transferring ferroelectric thin films to any type of substrate, but these result in costly process besides adding an enormous complexity to it. The crystallization temperature of ferroelectric thin films can be reduced by their direct growth on a seed layer of a dissimilar material displaying the same crystalline structure (i.e., by lowering the activation energy for perovskite nucleation) (Chen G, Zhang). Buffer layers of dielectric $SrTiO_3$, $PbTiO_3$ and $SrRuO_3$, or conductive $LaNiO_3$ oxides have been employed to obtain $Pb(Zr_xTi_{1-x})O_3$ ferroelectric thin films at annealing temperatures close to 450 °C(Chen G, Zhang). However, it is worth noting that high temperatures (500-700 °C) are previously required to crystallize the seed layer on the silicon substrate, which ruins the efforts to not degrade the semiconductor transistor apart from increasing the complexity of the integration process. Particularly for lead- and bismuth-based perovskite films, a strategy used to decrease their preparation temperature consists in the incorporation of either PbO or Bi_2O_3 excesses, even up to 50 mol%, to the respective precursor systems (Chen G, Zhang). These compounds enhance (as a flux for crystal growth) the solid-state diffusion of elements during crystallization, leading to the formation of the ferroelectric crystal phase at lower temperatures with respect to stoichiometric samples (Chen G, Zhang). On the other hand, the evaporation of elemental Pb and Bi is known to

occur earlier (i.e., at lower temperatures) from the respective excess (amorphous) oxides rather than from the nominal perovskite phase. Volatilization of such species at these processing conditions results in the detrimental contamination of conventional circuits at the back equipment.

Apart from the former crystallization aids, the fabrication temperature of ferroelectric oxide films can also be reduced intrinsically to the chemical composition of the material candidate. Thus, the crystallization temperature of the PbO-ZrO_2-TiO_2 solid solution decreases as the Zr/Ti ratio is lowered (Ahmad et al., 2006). In other words, the Ti-rich compositions are the ones that can be crystallized at a lower temperature, with minimum values reported for ferroelectric $Pb(Zr_{0.30}Ti_{0.70})O_3$ films around 400°C(Ahmad et al.,2006). The former composition of tetragonal symmetry is at present the best material choice for the development of ferroelectric memories by companies. We must strengthen that $Pb(Zr_xTi_{1-x})O_3$ with a composition near the morphotropic phase boundary (MPB), namely $Pb(Zr_{0.52}Ti_{0.48})O_3$, displays a crystallization temperature between 500–700 °C that has historically hampered its preparation at temperatures suitable for the current CMOS technology. This material is certainly the ferroelectric with the greatest commercial applicability and the basis of the current high-sensitivity piezoelectric ceramics (Ahmad et al., 2006). Therefore, its fabrication at temperatures compatible with semiconductor devices would represent a major breakthrough in the field of nano- and microelectronics, covering a potential industry need for the coming years.

In this work, we demonstrate the high performance of $Pb(Zr_{0.52}Ti_{0.48})O_3$ (hereinafter, PZT) thin films grown on silicon substrates at 400°C, an annealing temperature consistent with the standard process followed in the semiconductor industry for embedding into logic circuits. A low-temperature solution method is used whereby neither modification of substrate heterostructure (by incorporation of seed layers) nor the addition of PbO excess is needed, thus avoiding technological drawbacks to the integration routine. The evaluation of the ferro-, pyro- and piezoelectricity of these low-temperature PZT films on silicon reveals the multiple functionality that this active layer offers in a wide range of advanced electronic devices such as FeRAMs, ferroelectric field effect transistors (FeFETs), uncooled infrared sensors, or micro/nano-electromechanical systems (transducers, actuators).

Generally, MOCVD provides high quality thin films. Nevertheless, there are two drawbacks. Firstly, there is the need to deal with toxic lead compounds in the vapour phase, and secondly these processes have rather low deposition rates of approximately 30 nm/h (Chen G, Zhang Y) up to 100 nm/h (Tiwari B,). In applying the reactive magnetron, sputter process oxygen is used as a reactive gas which can cause an oxidation of the metallic target (target poisoning). Therefore, the sputter- and deposition rate decreases by a significant amount in comparison to pure metal processes.

Deposition rates of about 100 nm/h (Yunxia Zhou) and 425 nm/h (Fengang Zheng) are reported. Besides these semiconductor equipment compatible techniques a lot of research into the field of non-standard semiconductor methods is in progress, for instance hydrothermal method (Zheng F), sol–gel techniques (Yarmarkin V), screen-printing (Ichiki M), pulsed laser deposition (Yao K,) and electrostatic spray deposition (Qin M,). However, these technologies are difficult to be implemented in silicon wafer lines or suffer from the quality of the layers. The way out of this dead end seems to be a rather well known technique in terms of mechanical engineering but a completely new technique in terms of MEMS-technology. Gas flow sputtering (GFS) is a modified sputter technique using a hollow cathode glow discharge. In the past, it was used to coat turbine airfoils, flat glass and other parts (Cao D,).

2.1. Gas flow sputtering

GFS is a relatively new coating technique, first published by Ishii et al. (Chen B,). It is a special PVD technique, based on a hollow cathode glow discharge and a gas flow driven material transport. In contrast to magnetron sputtering, the target is shaped into a hollow, either in form of a tube or of two rectangular, parallel plates, facing each other. In an appropriate pressure range which depends on the hollow cathode width, the discharge current increases up to three orders of magnitude, mainly due to the charge carrier confinement and merging of the negative glow from opposite cathode areas. This is called the hollow cathode effect. In the GFS sources, cathode width and operating pressure usually are some centimetres and 0.1–1.0 mbar, respectively. Due to the hollow cathode effect and the comparatively high operating pressure, a high power density can be realised, resulting in a high plasma density and an intense sputter erosion of the target. Thus, additional magnetic fields are not required.

The material transport is based on convection of the working gas (usually argon) which flows through the hollow cathode towards the substrate and contains the sputtered target material. In

cases of reactive film deposition, e.g. oxide films, the reactive gas is fed into the space between source and substrate, becoming activated there by the hollow cathode plasma (Ming Wu,). An additional task of the argon gas flow here is to displacing the reactive gas from the activated target surface and thus prevents the formation of insulating layers resulting in unstable plasmas.

The deposition of ternary or quaternary films by PVD is sometimes complicated due to strong differences in the vapour pressure of the elements or by their in miscibility making target manufacturing impossible. In such cases, GFS can be advantageous using targets composed of segments from pure elements.

The segments should be arranged along the gas flow direction resulting in a thorough mixing of the sputtered material during gas transport. Changing the size of individual segments, the film stoichiometry can be simply adjusted. This saves considerable time compared to experimentation using alloy targets.

In this work, a GFS source with a tubular target of 40 mm inner diameter and 60 mm total length was used. The target was composed of metal rings of lead and titanium of appropriate thickness. Granular composites that consist of ferroelectric ceramic particles randomly distributed in a polymer matrix are interesting candidates for demanding long term applications due to their ease of fabrication, tunable electroactive properties, high mechanical stability, versatile product size range, ease in making complex patterns and low manufacturing cost (Liu Y,). Moreover they can be flexible if properly selected polymer matrix material is used and the ceramic volume fraction is kept low. However below the percolation threshold there is no continuous path of the particles from one electrode to another. Therefore the poling efficiency as well as the electro-active properties strongly depends on the electrical conductivity of the polymer matrix. Recent investigations have shown that the electrical conductivity of the constituents has a significant effect on the dielectric, piezoelectric and pyroelectric properties of the granular composites. It has been reported that enhanced electrical conductivity of the matrix shortens the build-up time of the electric field acting on the ceramic particles thus leading to higher poling efficiency in those composites. Moreover the piezoelectric and pyroelectric properties of the composites also improve significantly (Fengang Zheng,). Among various kinds of commercially available ferroelectric ceramics for sensing applications lead titanate (PT) is regarded as a good pyroelectric material because of a large spontaneous polarization, small relative dielectric constant, and a large pyroelectric coefficient (Yarmarkin V,). Similarly PEO is a synthetic polymer currently used as an ionic conducting polymer for Li-batteries, displays,

sensors, and other electrochemical devices (Qin M, Yao K, Liang YC). The interesting properties of PEO are good structural integrity, low glass transition temperature, flexibility and biocompatibility (Qin M,). In the current study the dielectric, piezoelectric and pyroelectric properties of PT-PEO composites are investigated and compared with that of PT-epoxy composites to enlighten the effect of the electrical conductivity of the matrix on the sensitivity and poling efficiency of the composites.

2.1. Understanding the Photovoltaic Response of Ferroelectrics

Photoferroelectrics are the materials with the combined property of ferroelectricity and photovoltaicity. Ferroelectrics contain domain walls based on the directions of polarizations. Hence, the photovoltaic effect is due to the possible separation of electrons and holes at domain walls. When external field is applied to the ferroelectric, all the dipoles start orienting in the direction of field and hence the net dipole moment is produced. The regions across the crystal contain different dipoles oriented in different directions, called domains. These domains are assumed to be separated by domain walls. When an ac electric field is applied externally, the domain polarize in the direction of applied field. When all the domains are polarized in the direction of field, material shows maximum polarization i.e. saturated polarization. When the field is reduced to zero, there will be still some polarization within the material. This kind of polarization, in the absence of field, is called remanant polarization (Pr). Photovoltaicity can be described in two different mechanisms. One is the generation of electrons and holes, in semiconductors/dyes, with the absorption of light (photons). Other is the separation of electron and hole pairs, by the built in electric field (also called as the depolarization field). Basically, the operation/functioning/performance of photoferroelectrics can be assessed/judged by the ability of light absorption, Pr, Voc, Isc, depolarization field, type of poling, etc. The intense interest in ferroelectric based photovoltaics is due to the fact that the semiconductor based photovoltaics show limited Voc (Chen G,).This could be easily overcome by the photoferroelectrics. The photo-ferroelectric structure can be visualized, as shown in figure 2.1. The ABO3 strucutre of PZT can be found in one of or report (Tiwari B,). The structure is as follows: electrode-Ferroelectric layerelectrode, where one will be the top electrode and other will be the bottom electrode. Poling can be done in two ways. One is applying the voltage to bottom electrode, usually known as positive poling. Other is applying the voltage to top electrode, usually known as negative poling (Chen G,).

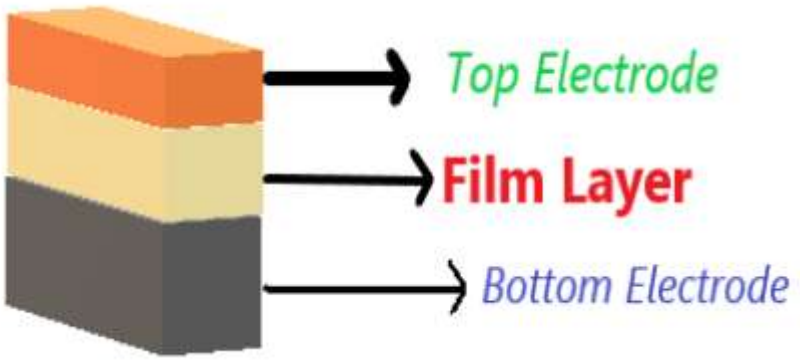

Fig. 2.1. Normal structure of Photo-Ferroelectric

In the structure, ferroelectric layer is responsible for the generation of electrons and holes. Also, it could produce an internal electric field (also called as depolarization field) which will be helpful in the separation of electrons and holes. Though they generate high open circuit voltages, the current induced by photons is observed to be very small. So, the performance of photoferroelectric devices should be enhanced to make them efficient and effective (Chen G,). In this report, we report the review on photovoltaic performance of ferroelectric PZT based photovoltaics. The photovoltaic properties such as Voc and Isc are summarized in numerous tables, for PZT of different compositions, and different structures. Because the structure can be changed with change in metal electrode, and hence altering the photovoltaic response. The metal electrodes, used mostly, are gold, platinum, silver, etc. One of the most used bottom electrode is In2O3 (ITO) substrate.

2.3. Ferroelectricity

Ferroelectrics are polar materials that possess a non-zero spontaneous electric polarization in the absence of an external electric field. By applying a suitable electric field, the polarization can be reoriented. A ferroelectric crystal is defined as a crystal which exhibits a spontaneous electric dipole moment. In other words, it means a crystal for which even in the absence of an applied electric field the center of positive charge does not coincide with the center of neg ative charges. So ferroelectrics are a class of polar dielectrics having permanentelectric dipoles oriented in a specific direction even in the absence of an external electricfield (Vijaya and R angarajan, 2004). Ferroelectricity was first discovered by Joseph Valasek in the year 1921 in s ingle crystal potassium-sodium tartarate tetrahydrate also known as Rochelle salt ($KNaC_4H_4O_6 \cdot 4H_2O$) which was then known as Seignette electricity. Later it was found to exist in polycryst

alline barium titanate($BaTiO_3$) ceramic by the mid 1940s (Nalwa,1999, Valasek,1971& Gene, 1999). Following the discovery of ferroelectricity in $BaTiO_3$, more ferroelectric materials wer e found, contributing to various applications commercially (Gene, 1999).

When an electric field (E) is applied to an insulator, polarization is induced into it, which forms an important parameter in the theory of insulators and hence when polarization is being investigated, dielectrics are included into this category (Jaffe et al., 1971). Classification of these materials based on their response in a realizable range of an electric field gives two types of dielectrics, linear and nonlinear. Linear dielectrics are dielectrics in which the electric polarization (P) varies linearly with the applied electric field (E), where a s it varies nonlinearly in the case of nonlinear dielectrics and the ferroelectric materials fall in to the latter category which can exhibit spontaneous polarization. Spontaneously polarized regio ns in ferroelectrics are known as domains. A suitably directed external electric field can be used to bring about a transformation from one state to another, which is a characteristic of ferroelect rics. Structurally speaking there are different types of ferroelectrics: Corner sharing Octahedra structures which includes: (the perovskite structured compounds, the tungsten-bronze group, bism uth oxide layer structured compoundsand lithium niobate and tantalate), Compounds containing H ydrogen Bonded Radicals, Organic Polymers and Ceramic Polymer Composites. Of these, the p erovskites (ABO_3) are by far the mostimportant category due to the wide range of the tolera nce factor, many different cationscan be substituted on both A and B sites without drastically ch anging the overall structure.

Complete solid solutions are easily formed between many cations, often across the entire range of composition. As a result, it is possible to manipulate a material's properties, such as C urie temperature or dielectric constant, and microstructures through controlled substitution of a given cation. Ferroelectrics have been categorized in the literature in different ways. Another a pproach of classifying them is as soft or hard. Soft ferroelectrics are water soluble, mechanic ally soft, and have low melting or decomposition temperature. Examples of these materials a re;Rochelle salt, some other tartarates, some sulfates, nitrates and nitrites.Most of these involve hydrogen bonding above a Curie temperature, "H" ions and bonds are distributed randomly in a non ordered fashion. At the Curie temperature the crystals transform from a disordered parael ectric structure to an ordered ferroelectric structure.The ordered structure has specific pairs of po

sitions the hydrogen ions can fit into to form the reversible dipoles.Other common sources of di poles in soft ferroelectric crystals are tetrahedral groupssuch as PO_4^{3+}. Hard ferroelectrics incl ude the oxides formed at high temperature. They are mechanically hard, and are not water-s oluble. Examples include $BaTiO_3$, $KNbO_3$, $CdNb_2O_6$, $PbNb_2O_6$, $PbTa_2O_6$, $PbBi_2Nb_2O_9$ and m any others. Many of the hard ferroelectrics contain a small highly charged cation (Ti^{4+}, Zr^{4+}, Nb^{5+}, Ta^{5+}) in an oxygen octahedron and have a similar ferroelectric mechanism to $BaTiO_3$. O thers contain asymmetrical ions with a"lone-pair" electron configuration; Examples are Pb^{2+}, Bi^{3+}, Sn^{2+}, Te^{4+}, I^{5+}. Each of these has two electrons outside a closed shell. These form a lone-pair orbital on one side of the ion and promote a directional bonding. The resulting structure has dipoles that result in spontaneous polarization when the dipoles do not cancel each other (R icherson, 1992). Another classification of ferroelectrics is based on the magnitude of atomic displacements and the resulting spontaneous polarization. Some crystals have atomic displace ment along a single axis (one-dimensional). Since the complete displacement in these crystals is concentrated in a single direction, the spontaneous polarization is high ($25\mu C/cm^2$). Examples in clude; $BaTiO_3$, $PbTiO_3$, $LiNbO_3$, SbSI, and Bi_2WO_6. Atomic displacements in some crystals are along planes (two-dimensional). The spontaneous polarization is only $5\mu C/cm^2$. Examples incl ude $BaCoF_4$, HCl, $NaNO_2$. Ferroelectrics with tetrahedral groups or hydrogen bonding have co mplex structures with three-dimensional effects on polarization. Spontaneous polarization is less than $3\mu C/cm^2$) (Richerson, 1992).

2.3.1. Properties of ferroelectric materials

Ferroelectric material is a material that has over a certain temperature range spontaneous polarization that can be reversed or reoriented by application of sufficiently large external electric field. The displacement of cations and anions gives rise to dipole moments within each unit cell and the resulting polarization can be measured via the material's surface charge density. Generally a ferroelectric has one or more polar axes along which a spontaneous polarization can be developed below the material's Curie temperature. One distinctive characteristic of ferroelectric materials is the hysteretic behavior in the polarization vs. electric field curve.

2.3.1.1. Ferroelectric hysteresis

Applying a variable electric field to a ferroelectric will result in a hysteresis loop similar in a ferromagnetic metal as seen in figure below. Ferroelectric crystals possess regions with

uniform polarization called ferroelectric domains. Within a domain, all the electric dipoles are aligned in the same direction. There are many domains in a crystal separated by interfaces called domain walls. Ferroelectric single crystals, when grown, have multiple ferroelectric domains. A single domain can be obtained by domain wall motion made possible by the application of an electric field. A very strong field could lead to the reversa l of the polarization in the domain, known as domain switching (Ahmad et al., 2006). Key characteristic of a ferroelectric crystal is that the direction of the polarization can be reversed by application of an electric field and that hysteresis loops result. The ferroelectric domains are randomly oriented prior to application of the electric field, that is at E=0 and the net polarization is zero (P_{net}=0). As an electric field is applied, and upon increasing this electric field the domains begin to move and align parallel to the applied field. This re sults in increase in net polarization along the applied field direction. The polarization reaches a saturation value (III) when all the domains are aligned in the direction of the field. If the electric field is reduced to zero, many of the domains will remain aligned such that a remanent polarization (IV) exists. If the electric field is reversed, the domain will switch direction.When enough domains switch, the domains in one direction balance the domai ns in the opposite direction and result in zero net polarization. This occurs for an electric field called the coercive field (–Ec). Continued increase in the negative electric field causes net polarization in the opposite direction, reaching the point VI where all the available domains are aligned. For instance, Maximum alignment of domains can be achieved by cooling the $BaTiO_3$ crystal through the 120°C.

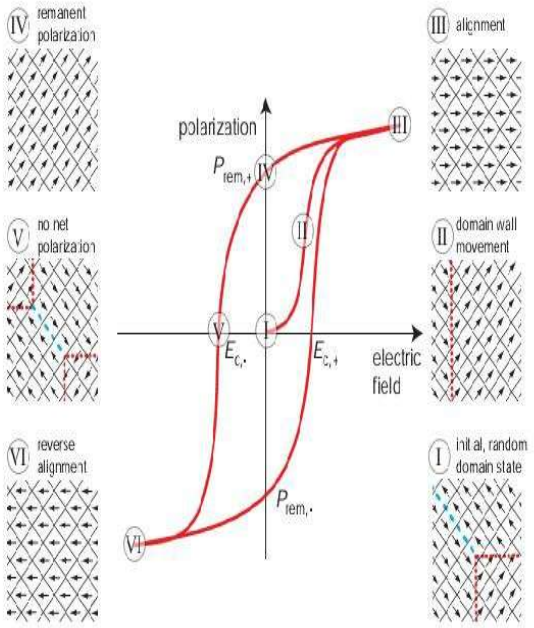

Fig2.2.Schematics polarization hysteresis

Shape of the hysteresis loop varies for different temperatures below the Curie temperature as shown in figure below. It gets thinner as the temperature increases and becomes single line above Curie temperature when the material is no longer ferroelectric. A ferroelectric behavior is dependent on the crystal structure. The crystal must be noncentric and must contain alternate atom positions or molecular orientations to permit the reversal of the dipole and the retention of polarization after the voltage is removed. Generally see figure2.2 (Richerson, 1992).

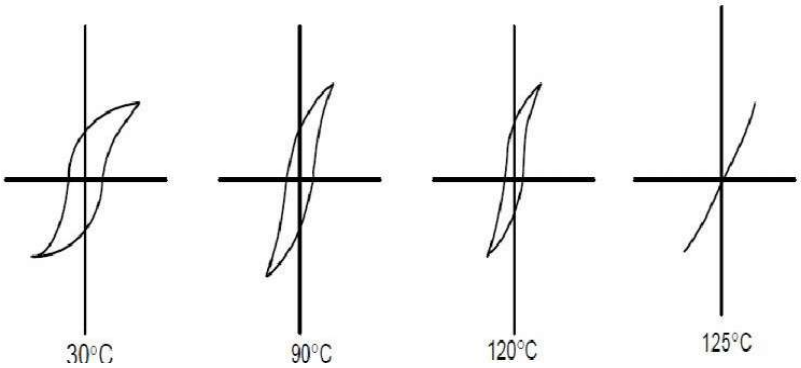

Figure2.3. Change in the hysteresis loop shape for $BaTiO_3$ at various temperatures

2.3.1.2. Ferroelectric domain

Small region of the material with same polarization orientation is referred as ferroelectric domains. When the sample is under zero field and strain-free conditions, the entire domain st

ates have the same energy. But if an electric field is applied, the free energy of the system is lowered by aligning the polarization along the field. The process of applying electric field to ferroelectric materials in order to orient the dipoles in the same direction is called poling. Thus, large applied electric field can permanently reorient polarizatio n between the allowed domain states which are restricted by crystallography. As a result, even ceramics constituted by polycrystals randomly oriented can be electrically poled to produce net piezoelectric coefficients.Much of the importance of ferroelectric materialsis d ue to their properties leading to a wide range of applications. Among these application, high di electric constant capacitors, piezoelectric sonar, ultrasonic transducers, ultrasonic motors, actuat ors and pyroelectric detectors. See figure 2. 3 (Dittmer, 2012).

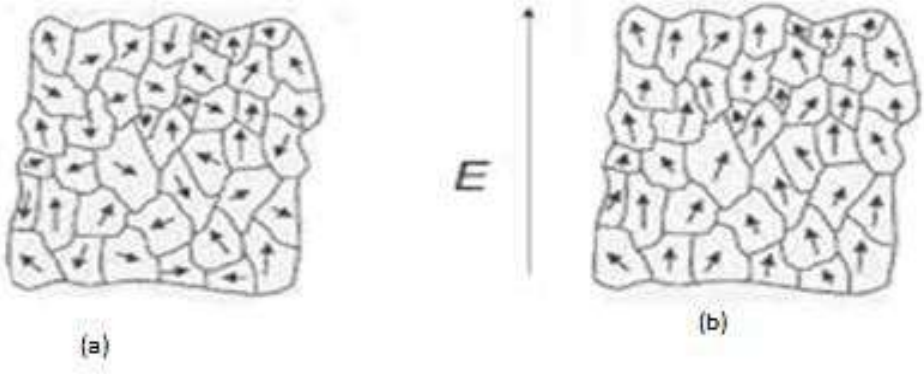

Figure2.4 (a) Domains & (b) poled domains electric dipole

2.3.1.3. Perovskite structure

Among all the structures, perovskite type (ABO_3) oxides have gained much attention as having many excellent physical properties such as ferroelectrics, piezoelectrics, magneto electric and electro optic effects (Shukla and Choudhary, 2010). The main advantage of the perovskite structure is that, many different kinds of cations can be substituted on both A and B-sites without drastically changing the overall structure and also complete solid solution can be achieved between many cations over a range of composition. The mineral perovskite is calcium titanate, with chemical formula $CaTiO_3$; its ideal structure has space group Pm-3m. Most of the commercially important ferroelectric materials have perovs kite related crystal structure. The family of the perovskite oxides has generic compositionABO_3, where "A" stands for a large cation such as Pb^{2+} (ionic radius of 1.19Å), Na^{1+} (ionic radius of 1.38Å), Bi^{3+}(ionic radius of 1.03Å) Ca^{2+}, Sr^{2+}, Ba^{2+},etc and "B" for a small cation such as

Mg^{2+} (ionic radius of 0.72Å), Nb^{5+} (ionic radius of 0.69Å),Ti^{4+}(ionic radiusof 0.61Å), Zr^{4+}, Z n^{2+}, etc. The coordination number (CN) is 12 for A-site cations and 6 forB-site cations. For e ach oxygen ion (O^{2-} (ionic radius 1.4Å), there are four A-site and two B-site cations directly b onding to it.The most commonly studied ferroelectricshave the cubic perovskite structure (in the paraelectric state) with a generalchemical formula ABO_3. As shown in figure below, A-si te cations occupy the corners of the cube while B-site cations site in the center of the oxygen octahedra.Oxygen occupies the face centers of the cube.A Perovskite is centrosymmetric where A-site cation valence varying from +1 to +3 and B-site is occupied by the cations of valence +3, +4 or +5. The lattice constant of the perovskite primary unit cell is always close to 4Å due to the rigidity of the oxygen octahedral network and the well defined oxygen ionic radius o f 1.40Å (Shannon, 1976). Goldschmidt's tolerance factor is an indicator for the stability and dis tortion of crystal structures. It is given as follows:

$$t = \frac{RA+RO}{\sqrt{2}(RB+RO)} \quad \text{----------2.1}$$

Where, RA-ionic radii of A-site cation, RB- ionic radii of B-site cation and RO-ionic radii of oxygen anion. For ideal perovskite system, *t* tends to be is about 0.95-1.0, for cubic symme try and larger for the distorted perovskite structure like tetragonal, rhombohedral structures etc. but non perovskite if is slightly less than 0.95 (Wood, 1951). The normal ferroelectric phase becomes stabilized as the value of *t* increases. Example, $CaTiO_3$ is cubicwit h t=0.97, $SrTiO_3$ is cubic with t=1.00 and $BaTiO_3$is tetragonal with t=1.06 at roomtemperature. A practical advantage of the perovskite structure is that due to the wide range ofthe toleran ce factor, many different cations can be substituted on both A and B sites without drastically changing the overall structure.Complete solid solutions are easily formed between many cati ons, often across the entire range of composition.

As a result, it is possible to manipulate a material's properties, such as Curie temperature ordiel ectric constant and microstructures through controlled substitution of a given cation. see figure2.14(Luo, 2005).

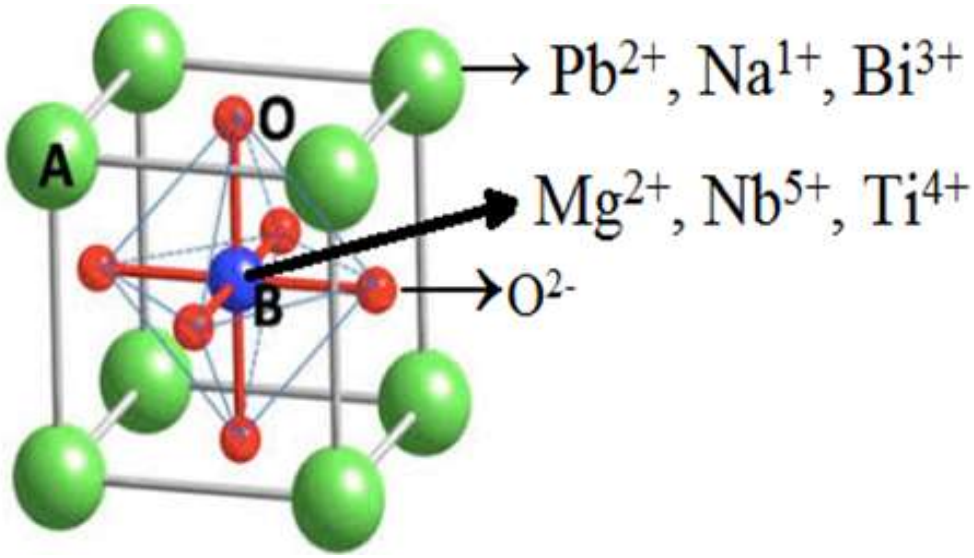

Figure2.3.The perovskite structure ABO_3

The perovskite type structure is enormously tolerant to variations in composition and distortions due to its ability to adapt (adjust) a mismatch between the equilibrium A-O andB-Obond lengths, allowing the existence of a large number and variety of stoichiometric compounds. Those distortions, for instance tetragonal, orthorhombic, rhombohedral and monoclinicgive rise to changes in the crystal symmetry and one or more cations shiftfrom high symmetry positions in the lattice producing ferroelectric or antiferroelectric behavior.In otherwords, the center of positive and negative charge within the unit cell is no longer coincidentwhich is the origin of the spontaneous polarization. However, in a ferroelectric material the spontaneous polarization is necessary but not sufficient, since it also requires the reorientation of the polarization by an electric field.

2.4. Phase Transition in Ferroelectric Materials

There are two types of causes for ferroelectric phase transitions, a displacive phase and order-disorder transitions (Lines and Glass, 1977). The displacive transition is a transition in which an ion is displaced from equilibrium position by experiencing the force from local electric field due to the ions in the crystals increases faster than the elastic restoring forces. This leads to an asymmetrical shift in equilibrium ion positions and hence to a permanent dipole moments. Example, ionic crystals such as barium titanate ($BaTiO_3$) exhibites displacive ferroelectric transition. One of the order disorder types of ferroelectrics is the existence of random dipole moment in each unit cell at high temperature. At high temperatures

these dipoles are in random directions and lowering the temperature there will cause a phase transition hence the dipoles orderly arranged and within the domain all the dipoles are pointing towards the same direction. Example, hydrogen bonded ferroelectric materials. Compositional order-disorder is another type of order-disorder ferroelectric transition . Compositional disorder is the common features of relaxors which is the disorder in the arrangement of different ions on the crystallographic sites. The relaxor behavior due to the disorder of non-isovalent ions was first observed in the perovskite compounds for inst ance, $PbMg_{1/3}Nb_{2/3}O_3$(PMN) (Smolenskii et al.,1961)and $Pb(Sc_{1/2}Ta_{1/2})O_3$(PST) lead scandiu m tantalate. In which Mg^{2+}, Nb^{5+}, Sc^{3+}, Ta^{5+} ions are fully or partially disordered in the B-sub lattice of ABO_3 perovsktes. Substution of ions in A and B siteof the ABO_3 perovskite with different polarizabilities, valence state and ionic size will sufficiently produce (strain) dipolar diffects. it can leads to high degree of disorder to break the transilational symmetry there prevent formation of the long range order but this support the formation of local ordering (shortrange order)/PNR to introduce the relaxor properties. In all mixed metal perovskites the major driving force responsible for cation ordering is derived from the difference in the size and charge of the B-site ions. Pb (B'B") O_3 is the general formula for the complex perovskite with multiple cations at B-site (Hilton et al., 1990). By adopting an arrange ment with positional order, electrostatic interactions between the cations (means cation-cation coulombic interaction) are minimized, and the intermediate oxygen anions can undergo conce rted (intensive) displacements to positions that accommodate the different equilibrium bond lengths of the octahedral cations (Davies &Akbas, 2000). For example in $Pb(B'_{1/3}B''_{2/3})O3$, due to the larger ionic size and lower valence of Mg (0.72Å for Mg^{2+} vs. 0.64Å for Nb^{5+}), both size and charge difference between B′ and B″ sublattices increased si gnificantly (Juhas & Davies, 2004).

According to (smolenskii et al., 1959) believe, in PMN the relaxor properties is due to compositional fluctuation which raises local field variation. The molar ratio of B^1 to B^2 cations depend on their valences & should be chosen in such a way that no vacancies are created. Typical relaxor materials with a B site ratio of B^1: B^2 =1:2 are $(PbMg_{1/3}Nb_{2/3})O_3$) (PMN),$Pb(Ni_{1/3}Nb_{2/3}O_3)$(PNN) and $Pb(Zn_{1/3}Nb_{2/3})O_3$) (PZN) but the ferroelectric relaxor material PMN-PT is the most common system. Materials with a B-site ratio of 1:1 are obtained by substituting the $B^{1(2+)}$cation by higher valence cation such as Mn^{3+}or Sc^{3+}, which l

eads to compositions such as $Pb(Mn_{1/2},Nb_{1/2})O_3$, $Pb(Sc_{1/2},Nb_{1/2})O_3$, or $Pb(Sc_{1/2},Ta_{1/2})O_3$ (PST). Ferroelectric materials undergo first order or second order phase transition where asrelax or ferroelectric undergoes diffused phase transitions (DPT).The first order phase transition is ch aracterized by discontinuous reduction of spontaneous polarization at T_C. But the second ord er phase transition characterized by gradual reduction of spontaneous polarization with increa se in temperature and become zero at T_C. There is a difference among the three types of pha se transions namely first order (common in normal ferroelectrics), second order (common in normal ferroelectrics) and diffused phase transitions (common in relaxor ferroelectrics) as depicted in figure 2.5 below. The ferroelectric phase transition canbe t hermodynamical first or second order and involves a macroscopic symmetry change at T_C and t he transition is sharp and frequency independent. However, there is no structuralp h a s e transiti on across T_m in relaxor ferroelectric and the transition is broad and frequency dependent.see figure 2.5 (Burfoot & Taylor, 1979).

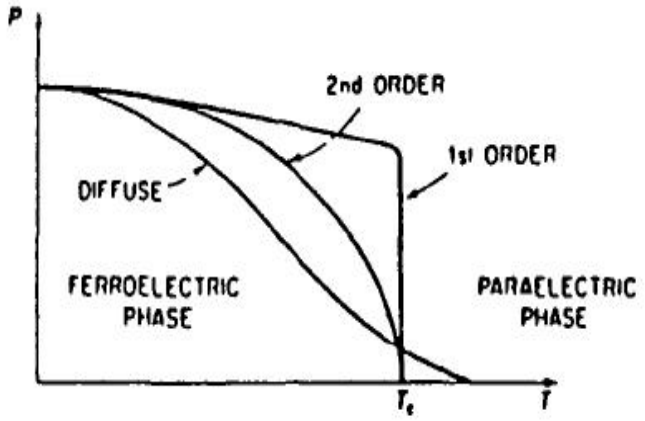

Figure2.4. Remanent Polarizations versus Temperature

2.5. Lead Magnesium Niobate (PbMg1/3Nb2/3O3)(PMN) & Its Solid Solutions

Research on relaxor ferroelectrics and related materials has undergone an accelerated growth bot h in fundamental understanding of the structural and physical properties and in practical applicati ons. PMN and its characteristic behavior were discovered several decades ago.

Smolenskii and Isupov first interpreted it as an indication of a "diffuse ferroelectric phase transition (Farber et al., 2002). Exceptional dielectrics & piezoelectric properties of members of th e $Pb(Mg_{1/3}Nb_{2/3})O_3$ family of relaxor ferroelectrics have led to extensive investigations of their synthesis, processing, properties, and structure in ceramic, single crystal, and thin film form. The c

omplex perovskite $Pb(Mg_{1/3}Nb_{2/3})O_3$ exhibit typical relaxor ferroelectric property (Cross,1994) ch aracterized by frustration/disturbance of local polarization due to composition and field in homogeneities, which prevents long range ferroelectric order from developing completely. From the structural point of view, the average symmetry of PMN when pro bed byconventional x-ray or neutron diffraction techniques, appears to be cubic(Pm3m)down to ver y low temperature with no evidence of macroscopic structural phase transition taking place through or below the temperature of maximum permittivity(T_{max}=265K), at 1kH) (Ye et al.,2002). PMN exhibits a broad, frequency dependent maximum of dielectricpermittivity an d possesses the cubic symmetry with the Pm3m space group in the entire temperature range (Sło dczyk et al, 2006). The PMN ceramic shows the low sintering temperature (≈1000^{o}c) which reduces its production cost. Efforts to optimize the dielectric constant of PMN ceramics have in the past focused on the elimination of a parasitic pyrochlore p hase. This has been partially achieved by a number of methods using excess MgO, precalcining the MgO and Nb_2O_5 oxides, using excess PbO and an optimum sintering cycle. T he PMN ceramics produced by these methods can, however, still have dielectric constants well below the single crystal value of approximately 20,000 (Guha,1985). Ferroelectric relaxor $Pb(Mg_{1/3}Nb_{2/3})O_3$ is known for more than five decades and is still in the focus of the rese arch as a prototypical example of relaxors. Complex perovskite $PbMg_{1/3}Nb_{2/3}O_3$ has been extensiv ely investigated since 1958 due to its unique relaxor ferroelectric behavior. Much of the experime ntal and theoretical research on relaxors has been focused on compositionally disordered perovskit es such as $PbMg_{1/3}Nb_{2/3}O_3$ and related compounds (Samara, 2003). Lead magnesium niobate was d iscovered shortly after the discovery of PZT. It is called a relaxor ferroelectric material because o f its dispersive (frequency dependent) dielectric response and diffuse phase transition (over a wid e range of temperature) around the Curie point T_{max} (temperature of the maximum dielectric perm ittivity) (Smolenskii,1970). PMN has the chemical formula $Pb^{2+}Mg_{1/3}{}^{2+}Nb_{2/3}{}^{5+}O_3{}^{2-}$ where there is a balance of the positive and negative charges. But any particular unit cell has either Mg^{2+} or Nb^{5+}at its body center. Thus there is a local deviation from the value +4 required for the occurrence of relaxor behavior leading to a Curie range of temperature rather than a single temperaturefor the occurrence of the ferroelectric transition. $Pb(Mg_{1/3}Nb_{2/3})O_3$ is a model relaxor system with the perovskite ABO_3 crystal structure, where the A-sites are occupied with Pb^{2+}an d the B-sites with $Nb^{5+}$and Mg^{2+}ions. As already explained, this material exhibits some

interesting properties, like a high dielectric permittivity, a large electrostrictive response, and a large piezoelectric activity when it is in a large enough DC field. Therefore, it is attractive f or capacitor & actuator applications (Setter, 2002). Addition of PT, it transforms through rhomboh edral, monoclinic to a tetragonal phase. In this system the morphotropic phase boundary (MPB) i s located near $Pb(Mg_{1/3}Nb_{2/3})O_3$ forms a solid solution with $PbTiO_3$ (PT), yielding relaxor-ferroe lectric (1-x)$Pb(Mg_{1/3}Nb_{2/3})O_3$-x$PbTiO_3$ materials (Ghasemifard et al,2010). One of the major problems concerning PMN-based materials is the difficulty in preparing them in a phase- pure condition (Heartling, 1999). Conventional solid state synthesis using a simultaneous mixing of constituent oxides usually yields in addition to the perovskite the pyrochlore phases. The latter deteriorate the dielectric, electrostrictive; ferroelectric and piezoelectric properties of the perovskite PMN based materials.

Adding to PMN the true ferroelectrics PT gradually changes its specific features. The increase in Ti content causes the changes of the phase transition nature from the relaxor into the normal ferroelectric one and makes possible the occurrence of the structural phase transitions of the different type. However, due to the high degree of structural and chemical disorder the behavior of the PMN PT system is very complicated. The presence of the polar nanoregions with distinct local symmetry as well as coexistence of phases with different symmetry causes t he difficulties in the unambiguous determining the structural properties. According to (Jaitanong et al.,2010) the solid solution of (1-x)$PbMg_{1/3}Nb_{2/3}O_3$-(x)$Bi_{1/2}Na_{1/2}TiO_3$ were formed by solid state reaction method. All compositions show complete perovskite solid solutio ns and the structure to change from cubic to rhombohedral at x=0.5. A Maximum dielectric con stant of 4343 were obtained at x=0.9 with diffused phase angle of γ= 1.99 indicating arelaxor ferr oelectric behavior for the sample. The temperature at maximum of the dielectric constant for the (1-x) $PbMg_{1/3}Nb_{2/3}O_3$-(x)$Na_{1/2}Bi_{1/2}TiO_3$ ceramics were seen to increase with i ncreasing NBT content. Moreover, the broadest dielectric peak occurs at x=0.9, which leads to a morphotropic phase boundary in this system (Suchanicza et al.,2017) found out that (1-x) $BaTiO_3$-x$PbMg_{1/3}Nb_{2/3}O_3$ ceramics prepared by solid state reaction have showed p-t ype conductivity. Low-frequency (20Hz-2MHz) ac conductivity obeys a power law which is c haracteristic for disordered materials. Both ac and dc conductivities showed a thermally activat ed character and possessed linear parts with different activation energies and someirregular chan ges. It was found that the hopping charge carriers dominate at low temperatur and small polaron

s and oxygen vacancies dominate at higher temperature. (1-*x*)$BaTiO_3$-*x*$PbMg_{1/3}Nb_{2/3}O_3$ ceramic s are expected to be promising new candidate for low-lead electronic materials.

2.6. Sodium Bismuth Titanate ($Na_{1/2}Bi_{1/2}TiO_3$)(NBT) & Its Solid Solutions

Sodium bismuth titanate or bismuth sodium titanium oxide (NBT or BNT) is a solid inorganic c ompound of sodium, bismuth, titanium and oxygen with the chemical formula of $Na_{1/2}Bi_{1/2}TiO_3$ or $Bi_{1/2}Na_{1/2}TiO_3$.This compound adopts the perovskite structure. $Na_{1/2}Bi_{1/2}TiO_3$ is not a naturall y occurring mineral and several synthesis routes to obtain the compound have been developed. It can be easily prepared by solid state reaction between Na_2Co_3, Bi_2O_3, and TiO_2 at temperatures a round 850^{o}c. The exact room-temperature crystal structure of sodium bismuth titanate has been a matter of debate for several years. Early studies in the 1960s using X-ray diffraction suggested $Na_{1/2}Bi_{1/2}TiO_3$ to adopt either a pseudo-cubic or a rhombohedral crystal structure (Smolenskii et al., 1961). In 2010, based on the high resolution single-crystal X-ray diffraction data, a monoclin ic structure (space group Cc) was proposed. On heating, $Na_{1/2}Bi_{1/2}TiO_3$ transforms at 533$\pm$5K to a tetragonal structure (space group P4bm) and above 793$\pm$5K to cubic structure (space group Pm 3m) (Zvirgzds et al., 1982). $Na_{1/2}Bi_{1/2}TiO_3$ is a relaxor ferroelectric. Its optical bond gab was rep orted to be in the 3.0-3.5eV (Bousquet et al., 2010). $Na_{1/2}Bi_{1/2}TiO_3$ (NBT) is one of the highly studied lead-free perovskite compounds for the replacement of lead-based piezoelectric ceramics on account of their potential electro mechanical properties. $Na_{1/2}Bi_{1/2}TiO_3$ and its solid solutions with other perovskites can have goo d piezoelectric properties and thus are considered to be the potential candidates for industrial applications. The intriguing phase transitions of both NBT and BNT-based solid-solutions as a function of composition and temperature make them an excellent model for studies on the phase transition behaviour (smolenskii et al., 1961). Various solid solutions with tetragonal ferroelectric perovskites including $BaTiO_3$ (Takenaka et al., 1991), $Bi_{1/2}K_{1/2}TiO_3$ (Sasaki et al., 1 999) have been developed to obtain morphotrophic phase boundaries to enhance the piezoelectric properties of $Na_{1/2}Bi_{1/2}TiO_3$. Pure NBT is an A-site complex perovskite structured ferroelectric with rhombohedral symmetry at room temperature. It has a high Curie temperature (Tc=320^{o}c) with strong ferroelectricity (Pr=38μC/cm^2)(Reichmann et al.,2015). However, the majordrawback with NBT is the poling treatment because of its high coercive field (Ec=7.3kV/m m), resulting in relatively weak piezoelectric properties (d33=70-80pC/N). Decreasing coercive field and improving the poling process formation of BNT-based solid solution with

a morphotropic phase boundary (MPB) is an effective way as proposed and studied by many rese archers. Theextra ordinarily large strain generated by a field induced phase transition in sodium b ismuth titanate based solid solutions prompted researchers to investigate its potential as an altern ativeto lead zirconate for actuator applications (Reichmann et al., 2015).

CHAPTER 3: MATERIALS AND METHODOLOGY

3.1. Materials

In one work (V. A. Chaudhari and G. K. Bichile), PbTiO3 (PT) was synthesis by solid state reaction. The conventional method of synthesizing PbTiO3 (PT) relies on the solid-state reaction between TiO2 and PbCO3 at high temperature. The conventional solid-state reaction has a tendency to produce a coarse PbTiO3 powder with compositional inhomogeneity and a degree of particle agglomeration if the processing parameters are not carefully optimized. Therefore, many chemistry-based processing routes, including co-precipitation [Qin M,], sol-gel synthesis (Qin M, Yao K and Liang YC (2008)), hydrothermal (Zheng F, Xu J, Fang L, Shen M and Wu X (2008)), and citrate routes (Cao D,), have been devised for the preparation of an ultrafine, sintering-reactive PbTiO3 (PT) powder. However, almost all these chemistry routes require calcination of the precursors at an elevated temperature to develop the desired PbTiO3 phase. Furthermore, most of these chemistry-based processing routes require high purity inorganic or organometallic chemicals as the starting materials, which are many times more expensive than the widely available oxides and carbonates. It has been observed that the synthesis of a mechanically robust, high density, monolithic ceramic pure PbTiO3 is not simple (Chen B,). Problems typically encountered include loss of lead (Pb) due to the volatility of PbO at elevated temperatures, porosity, and microcracking, in extreme cases leading to spontaneous fracture. The main hurdle in the PT fabrication is the synthesis of a single phase with required perovskite structure. The primary difficulty is due to the volatility of PbO at elevated temperatures. The PbTiO3 structure can only tolerate minor loss of lead (Pb), higher levels of which effectively promote second phase formation and the degradation of piezoelectric properties. An example is the formation of a PT phase with the pyrochlore structure observed during a co-precipitation synthesis experiment. A more common occurrence is the formation of a two-phase mixture with TiO2 (Ming Wu,). The volatilization of PbO is known to increase markedly at temperatures above 800◦C though the critical temperature is debated. Kim et al. (Yang Song,) have observed that a PbO-rich PT in liquid phase is formed above 838◦C, Alguero et al. (Amador P´erez-Tomas,) found that at 650◦C an excess of 20% PbO was required because of Pb-loss during thermal treatments of sol-gel prepared Lamodified PT thin films, whereas Ananta and Thomas (André Marino Gonçalves & José Antonio Eiras (2019)) found that Pb volatility in PMN-PT could be minimized by careful sintering up to 1250∘C. What is clear is that the loss of lead

depends on particle size of constituent oxides, processing conditions, and chemical stability. The degree of Pb incorporation into the presintered crystal structure affects the volatility enormously (Ming Wu,). Many groups report that loss of lead (Pb) may be minimized by sintering compacted powders in a surrounding lead-based powder or a PbO vapor atmosphere [Yang Song,] although this may lead to a Pb gradient in the final sintered product (Ming Wu,). The problem of porosity has largely been addressed through particle size control of the starting powder. Therefore, one of the aims of the present work is to optimize the processing parameters to obtain homogeneous, dense, crack-free samples using the conventional solid-state reaction method. A careful and systematic study optimization of the synthesis parameters provides an alternative means of minimizing the problem of cracking, porosity, and Pb volatility. Careful sintering at lower temperatures may restrict grain growth and on cooling internal strains are reduced. In addition, sintering at low temperatures, the problem of volatility of lead is minimized. It has been shown that homogenous powders with a fine grain size can be produced by the ceramic process on the optimization of synthesis parameters (Harshan VN,). The electrical properties result from the different contributions made from various components and processes present in the material, and complex impedance spectroscopy has been commonly used to evaluate and separate the contribution of the overall electrical properties in the frequency domain due to electrode reactions at the electrode/sample interface and migration of ions through the grains and across the grain boundaries in a polycrystalline material.

3.2. Methodology and procedures

$PbTiO_3$ (PT) samples were prepared by solid-state reaction processing using high purity oxide and carbonate as the starting materials, involving several steps such as mixing, wet grinding, calcination, and sintering along with intermediate grinding at each stage. Calcination at temperatures ranging from 450 to 550°C was carried out to synthesize the PT compound before sintering at different temperatures. Commercially available $PbCO_3$ (99.9% purity; Aldrich Chemicals) and TiO_2 (99.9% purity; Loba Chemie were used as starting materials. In order to compensate the loss of PbO during the high temperature sintering, 5% by weight excess of PbO was added. The excess PbO helps to compensate for the lead evaporation during sintering process. The polycrystalline samples of $PbTiO_3$ were prepared using the previous high purity ingredient materials in the required stoichiometry, and the powders were wet-milled. The sieved

fine powders were then calcined in the temperature range 450–550°C for 8 hrsders were again finely ground and sieved through a 75 m. The sieved powders were pressed in to pellets using polyvinyl alcohol (PVA) as a binder. The PT powders were then cold pressed into pellets of diameter 10 mm and thickness 1-2 mm at a pressure of 50 MPa using an isostatic hydraulic press. The pellets were sintered at four different temperatures 700°C, 750°C, 800°C, and 900°C for 12 hr. T he heating program was carried out using Carbolite programmable high temperature furnace with Eurotherm temperature controller. The phase structure of sintered specimens was investigated with X-ray diffraction.The X-ray diffraction data was collected over the scattering angle range $10^\circ \leq 2 \leq 80^\circ$at 2 step 0.02° using CuK (=1.5418A) radiations recorded at room temperature using X-ray powder diffractometer (Xpert Pro-PAN Philips). The morphological studies of all the sintered samples were carried out by using scanning electron microscopy (SEM). Samples were examined using a JEOL JSM-6360 A analytical scanning electron microscopy operated at 15 kV. For determining the average particle size from full width at half maximum (FWHM) the intensity of Bragg peak (101) was used. The density of the PT ceramic was measured using single pan balance and Archimedes principle. For electrical characterization, the sintered disks (900°C, 12 hrs) of PT samples were polished to make both the faces f lat and parallel and electrode with high-purity air-drying conducting silver paste. The impedance measurements were carried out using a computer-controlled impedance analyzer (HP 4192 A LF HEWLETT) over a wide range of temperature (33°C–560°C) and frequency (5 Hz–13 MHz) with an applied voltage of 1.3 V. Measurements provided the real and imaginary parts of the impedance and dielectric as frequency-dependent values.

In another work (Yarmarkin V,), Lead titanate thin films were prepared by the sol synthesis from acetylacetone/ethylene glycol route by a sol–gel method. For sol preparation, lead acetate (99.9% purity; Aldrich Chemicals, 3.123 g) was dissolved in ethylene glycol on reflux at 120°C for 1 h to decrease the residual water. Acetylacetone was used as the chelating agent to mix with titanium isopropoxide (99.9% purity, 5 ml), the molar ratio of acetylacetone/titanium isopropoxide being 4. The above solution was also refluxed at 120°C for 1 h and then about 15 ml of ethylene glycol was added to the acetylacetone/titanium isopropoxide solution. The above acetate solution was added to the titanium solution and refluxed at 120°C for 4 h, then 5 ml of deionized water was added for further hydrolysis and polycondensation until the solution becomes a sol and easy for spin coating. Prior to the deposition, the metallic substrates (stainless

steel (10 × 10 × 5 mm)) were thoroughly polished using zero fine grade (3/0) polish paper (supplied by Kohinoor Products, India) and then washed with liquid detergent followed by ultrasonic cleaning with double-distilled water. In order to remove oily substances from the surface, cleaned substrates were etched in 10% H2SO4 for 2 min and finally ultrasonically cleaned with double-distilled water.

The thin films were deposited by a spin coating technique by utilizing the as-prepared PT-sol (precoating 1,000 rpm for 10 s. followed by 4,000 rpm for 30 s.). The as-deposited film was then pyrolyzed on a hot plate for 5 min to evaporate residual organic species, respectively, for each layer deposition.

The deposition and pyrolysis procedures were repeated and then the films were finally annealed at various temperatures (200, 400, and 600°C) for 2 h, and a slow cooling rate of 2°C/min was used to avoid cracking of the films. In the case of thin films, film thickness (repeated by coating layers) and pyrolysis temperatures were studied systematically to investigate their influence on the formation of PT films. However, the coating layers and annealing temperature were 1–6 and 200-600°C, respectively. Figure 1 shows the schematic diagram of lead titanate using the sol–gel technique. The crystal structure and orientation of the PT films synthesized on stainless steel substrates were examined using an X-ray diffractometer (Xpert Pro-PAN Philips) with Cu–Kα radiation source. The surface morphology was studied using scanning electron microscopy (SEM, JEOL JSM-6360 A). For determining the average particle size from full width at half maximum (FWHM), the intensity of Bragg peak

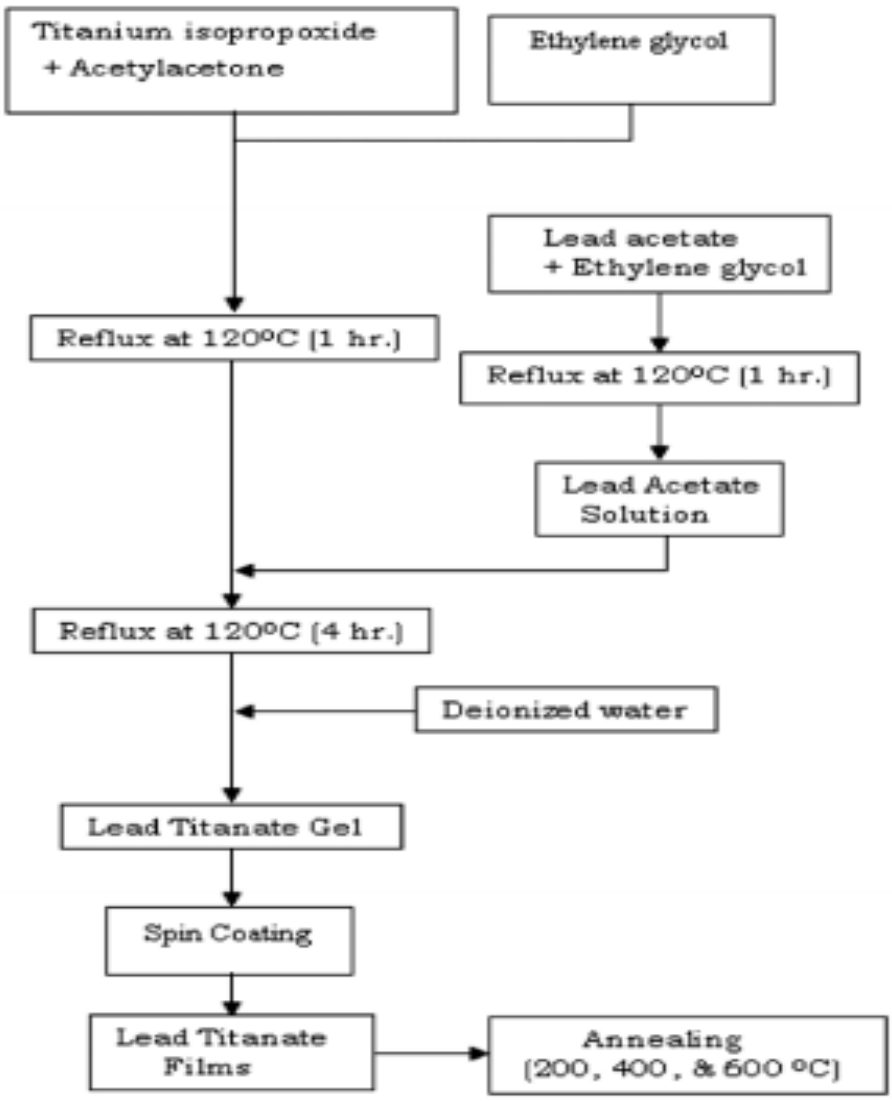

Figure 3.10. Schematic diagram of lead titanate using the sol–gel technique

In another work, it is well known that Pb diffuses into Si and reaction to PbSi can occur (André Marino Gonçalves & José Antonio Eiras (2019)). This silicate compound can modify the structure and surface of silicon. To avoid this damage a diffusion barrier of thermal oxide, Si_3N_4 and high temperature oxide (HTO, SiO_2) is used on silicon wafer substrates. These three layers are created in a A400^{TM} vertical oven supplied by ASM. Due to the small lattice mismatch and the inert behaviour of Pt it is quite common to use Pt as bottom electrode. To improve the adhesion of Pt, it is recommended (Anoop G,) to use Ti as adhesion layer.

CHAPTER 4: REVIEW OF RESULTS

4.1. Structural and Micro structural Characterization.

X-ray diffraction patterns collected at room temperature for the samples sintered at 700°C, 750°C, 800°C, and 900°C are shown in Figure 1. All the observed peaks/reflections are indexed in tetragonal crystals systems on the basis of the best agreement between observed and calculated interplaner (*d*) values. The values of unit cell parameters (*a, c*) and axial ratio (*c/a*) and density are given in Table 1. The comparative behavior of the tetragonality and unit cell volume with sintering temperature is shown in Figure 2, and the density variation with sintering temperature is shown in Figure 3. Figure 3 shows the measured and X-ray density(ρ_m,ρ_x) as a function of a sintering temperature. A slight increase in density is observed as sintering temperature increases up to 900°C. However, a density jump occurs at 750∘C, and almost dense ceramics are achieved thereafter. The results are shown in Figure 3.

Table 1: Unit cell parameters and *c*/*a* ratio of PT powder samples sintered at different temperatures.

Sintering temperature (°C)	*a* (Å)	*c* (Å)	*c*/*a* ratio	Density (X-ray) (g/cm^3)	
				ρ_x	ρ_m
700	3.9008	4.067	1.0426	6.91	6.09
750	3.9013	4.0673	1.0425	7.85	7.18
800	3.9032	4.0679	1.0422	7.91	7.35
900	3.9023	4.0657	1.0419	7.97	7.43

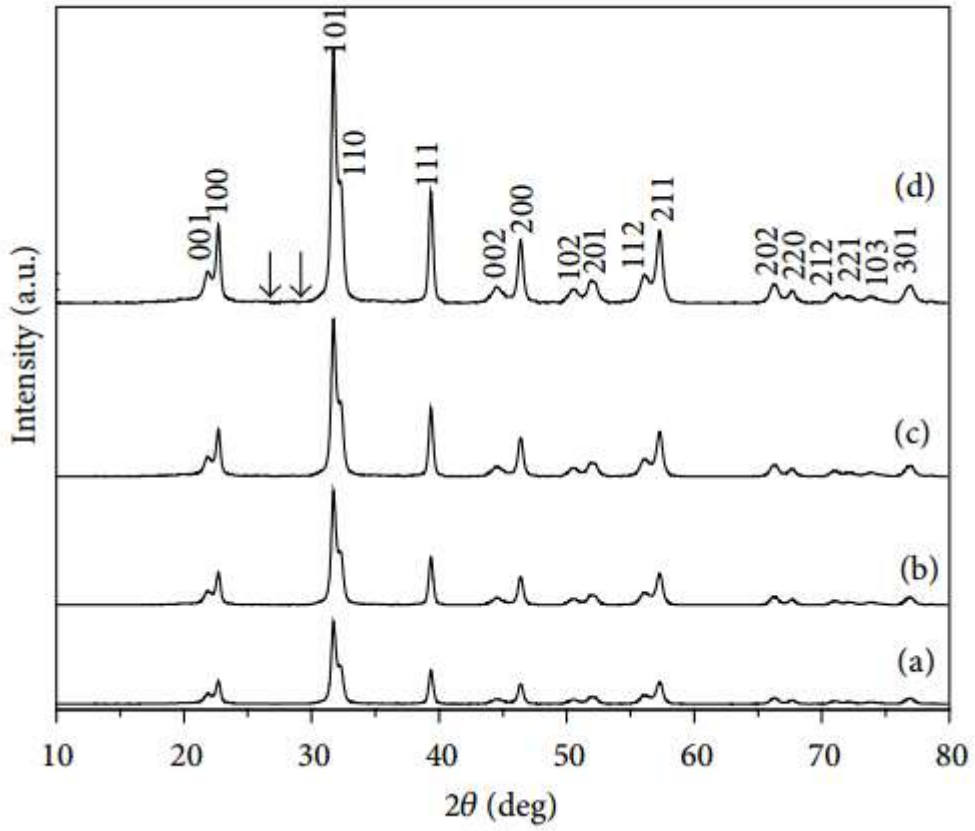

Figure 4.1: X-ray diffraction patterns of PbTiO3 (PT) sample sintered at different temperatures ((a) = 700°C, (b) = 750°C, (c) = 800°C, and (d) = 900°C).

The powder diffraction peaks from sample sintered at different temperatures showed that all the samples possess single-phase perovskite structure. The diffraction peaks have narrowed substantially with the increasing sintering temperature and the PT phase has persisted without evidence of second phase formation. Sintering athigher temperatures does not appear to substantially alter the nature of patterns. However, the XRD pattern collected at the highest temperature 900°C, Figure 1(d), shows additional minor diffraction peaks, suggesting the beginning of the evolution of second phase (indicated by arrow). Figure 4.1 shows the XRD patterns for the samples that have been sintered at 900°C for various time periods (4, 8, and 12 hrs). Fine perovskite PbTiO3 crystallites, as indicated by the peaks at 2θ angle of 21.8°, 22.5°, 31.6°, 39.1°, 44.5°, 46.0°, 50.5°, 51.5°, 55.9°, and 56.9°, were observed, together with much weakened and broadened peaks of TiO2 when the samples were subjected to for 4 hr sintering. This observation indicates that sintering at 900°C for the first 4 hrs triggers the formation of perovskites PbTiO3 phase, and at the same time, the peak broadening of

TiO2 implies that the first sintering has led to a significant refinement in the particle and crystallite sizes. The PbTiO3 phase was observed further when the sintering was extended to 8 hrs, which indicates that the formation of PbTiO3 phase occurred at the expense of constituent oxides with increasing sintering time. PbTiO3 was the only phase that was observed in the X-ray diffraction pattern in the sample that was sintered for 12 hrs The average particle size has been determined from the full width at half maximum (FWHM) of 101 peak using Scherrer's equation

$$t = \frac{0.9\lambda}{B\cos\theta_B},$$

where t is the particle diameter, λ the X-ray wavelength, B the FWHM of a diffraction peak, and θ_B the diffraction angle. The value of FWHM includes errors from the apparatus conditions such as the slit width of the X-ray diffractometer and these errors were corrected. The results were supported by the SEM micrograph studies. Figure 5 shows the variation of average particle sizes as a function of sintering temperatures determined from the peaks in the inset figures. Figure 6 shows the typical SEM pattern of PbTiO3 sample sintered at 900°C for 12 hrs. The pattern shows that the PbTiO3 particles have a more or less spherical morphology and consist of particle agglomerate of varying size, and the sizes of the grains are in the range 500 to 600 nm. The particle size (XRD), grain size (SEM), and phase and space group are listed in Table 2.

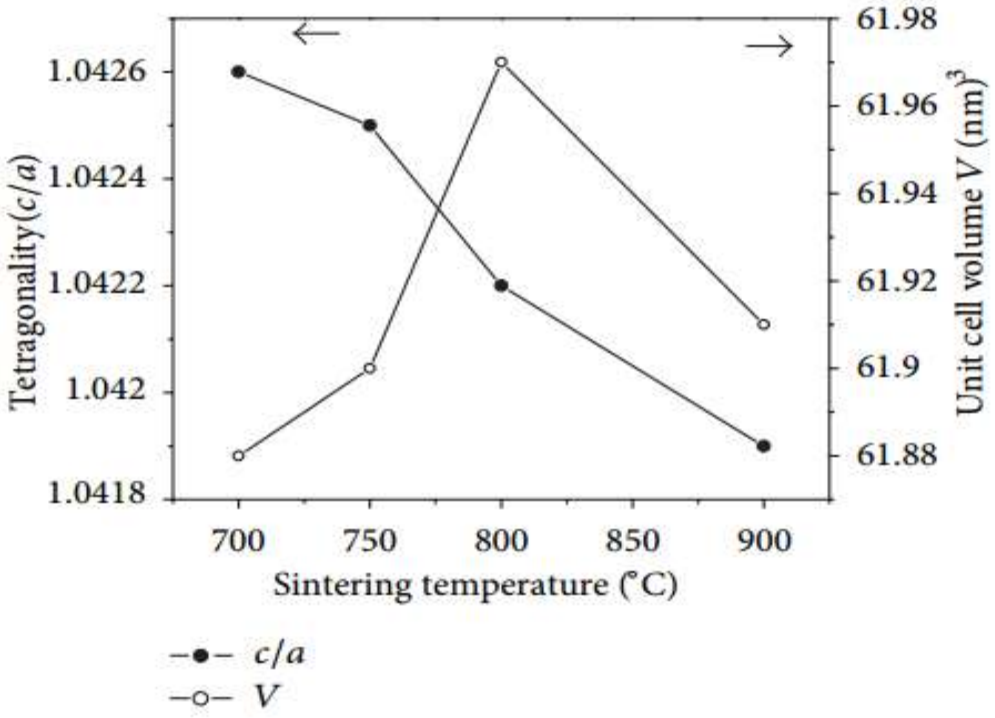

Figure 4.2: Variation of *c/a* and unit cell volume (V) with sintering temperature (◦C).

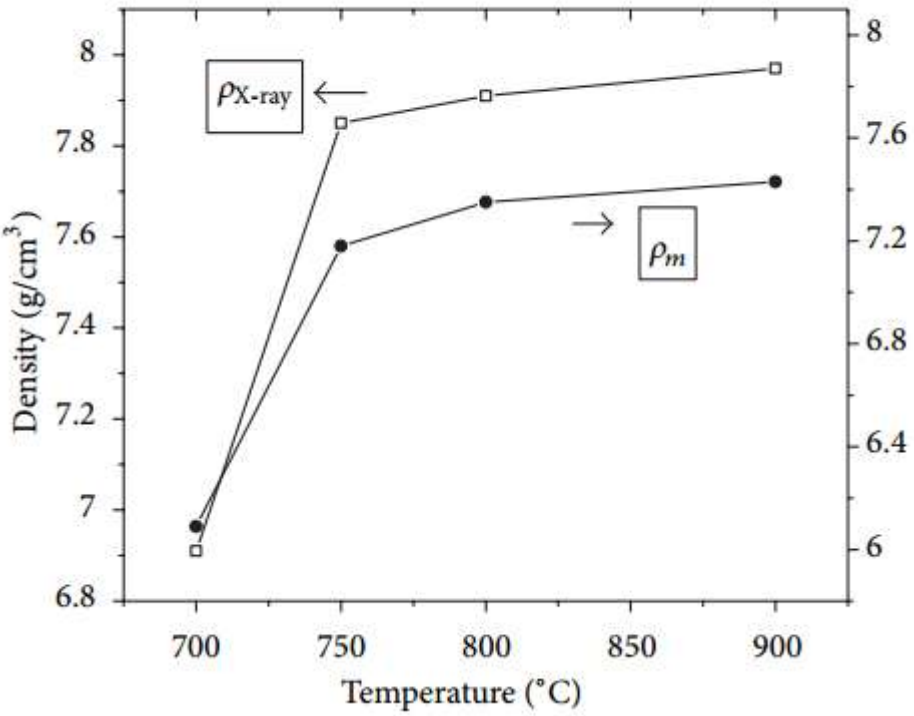

Figure 4.3: X-ray and measured density of the PbTiO3 (PT) ceramics as a function of sintering temperature.

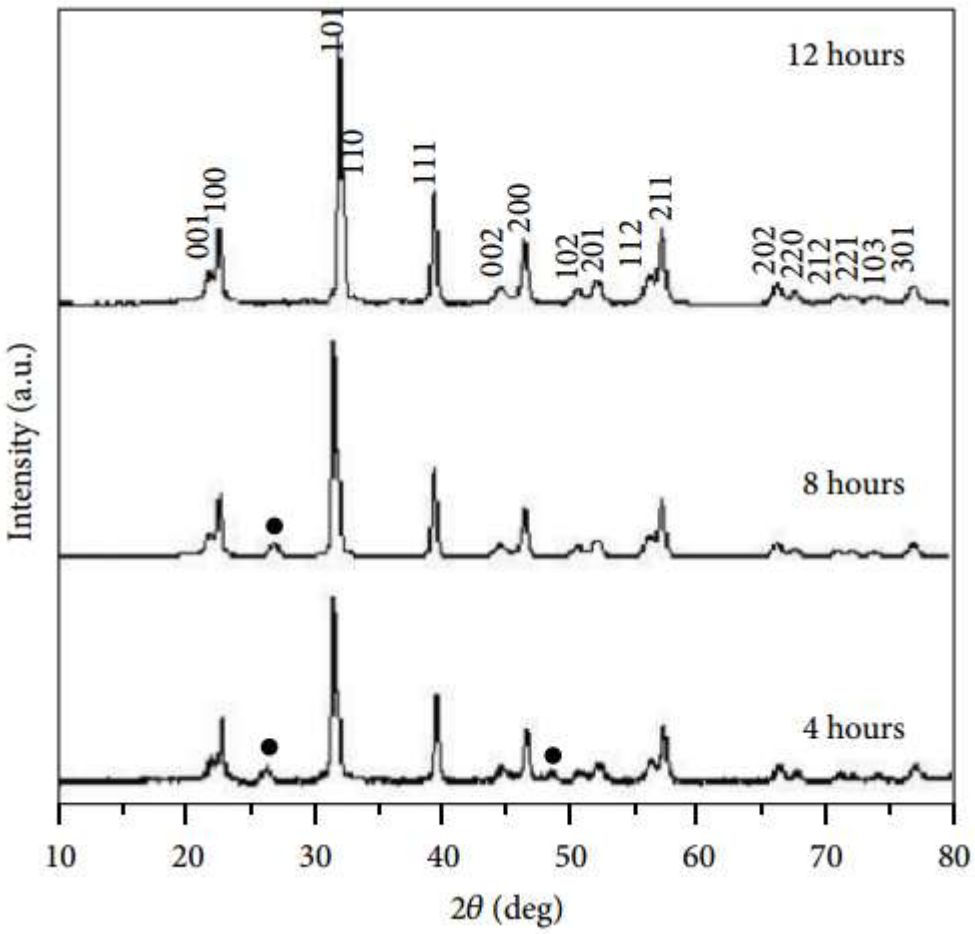

Figure 4.4: X-ray diffraction patterns of PbTiO3(PT) sample sintered at 900°C for various time durations (4, 8, and 12 hrs).

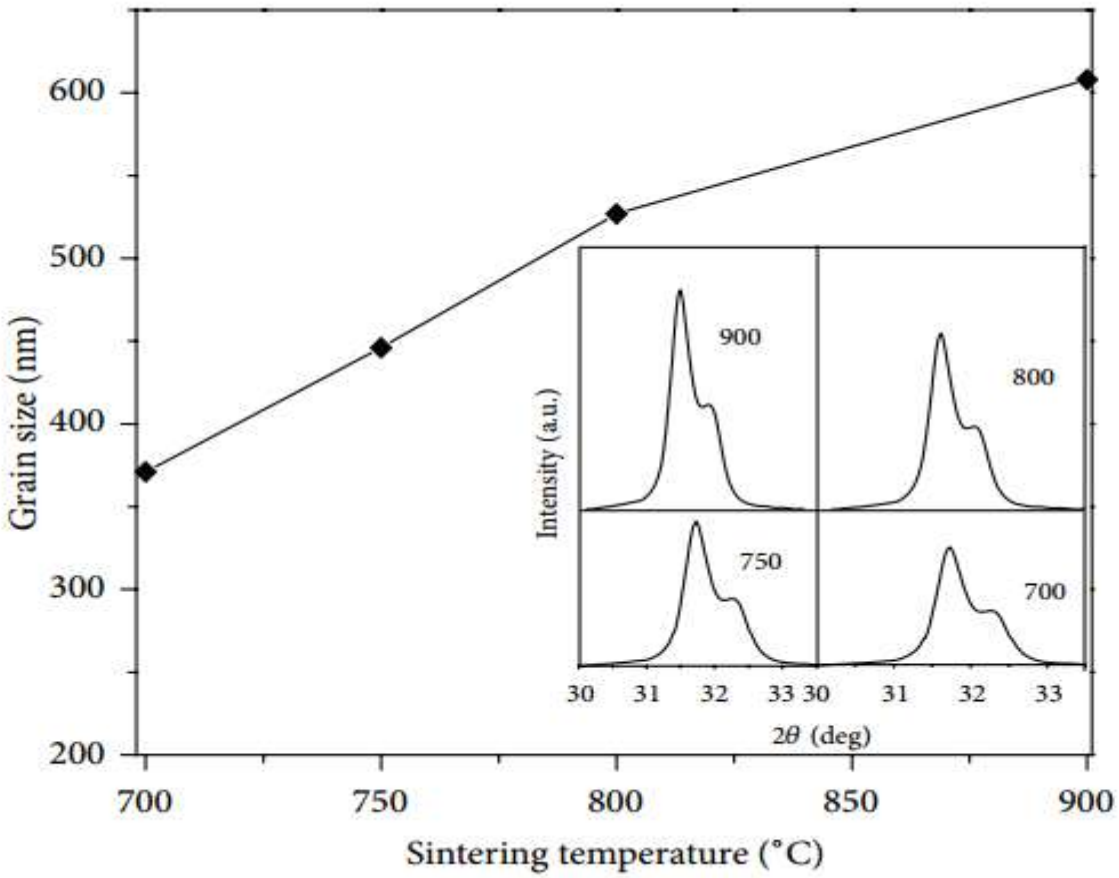

Figure 4.5: Particle sizes as a function of sintering temperatures. Figure in the inset shows the (101) peak. FWHM values were calculated from the Gaussian fits (solid lines).

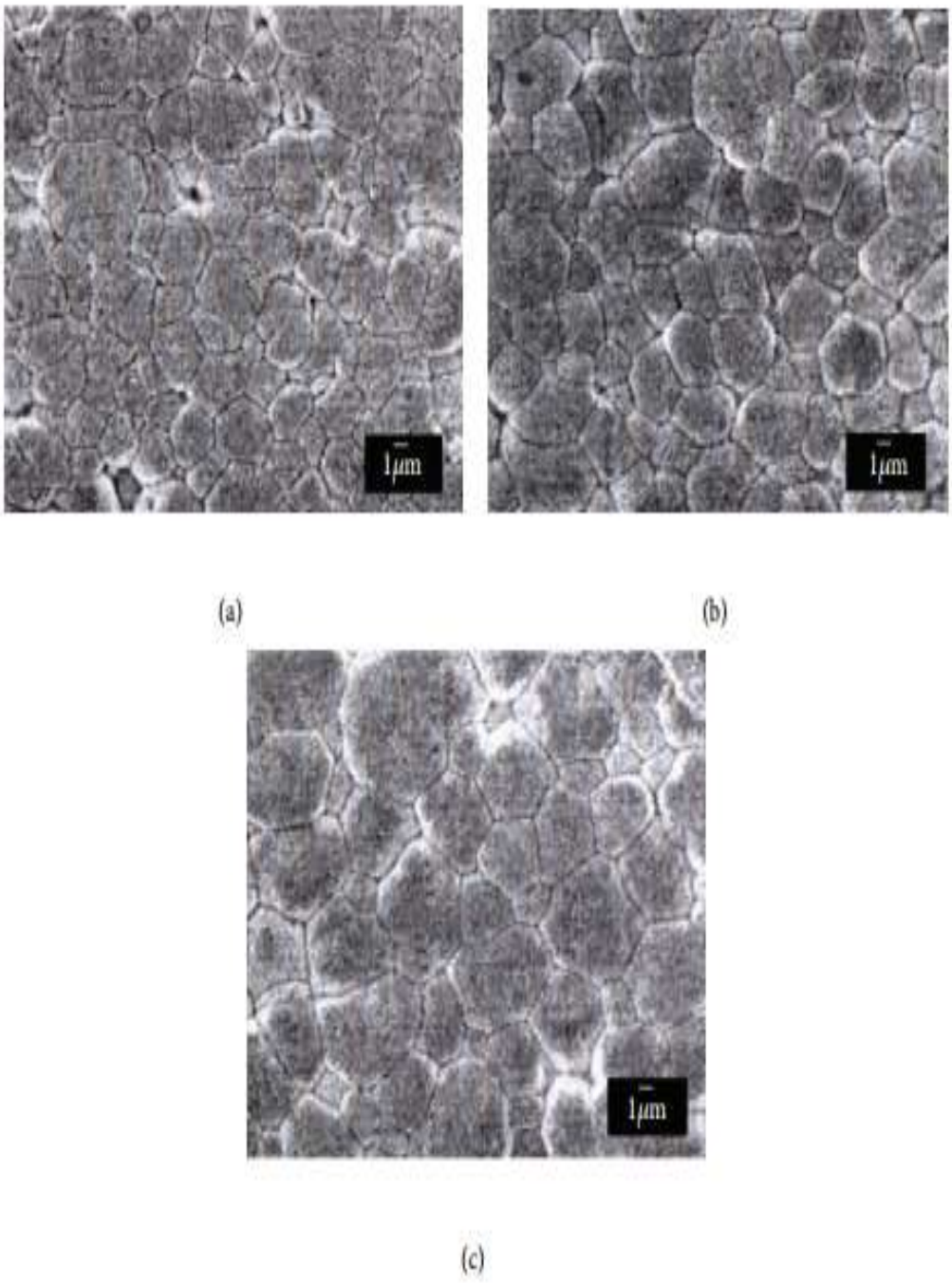

Figure 4.6: SEM micrograph for sample sintered at (a) = 750°C, (b) = 800°C, and (c) = 900°C for 12 hrs.

Sintering temperature (°C)	Particle size (nm)	SEM (nm)	Phase and space group
700	371	450	T (P4 mm)
750	446	540	T (P4 mm)
800	527	670	T (P4 mm)
900	608	883	T (P4 mm)

Table 2: Particle size (XRD), grain size (SEM) and phase and space group of PbTiO3 (PT).

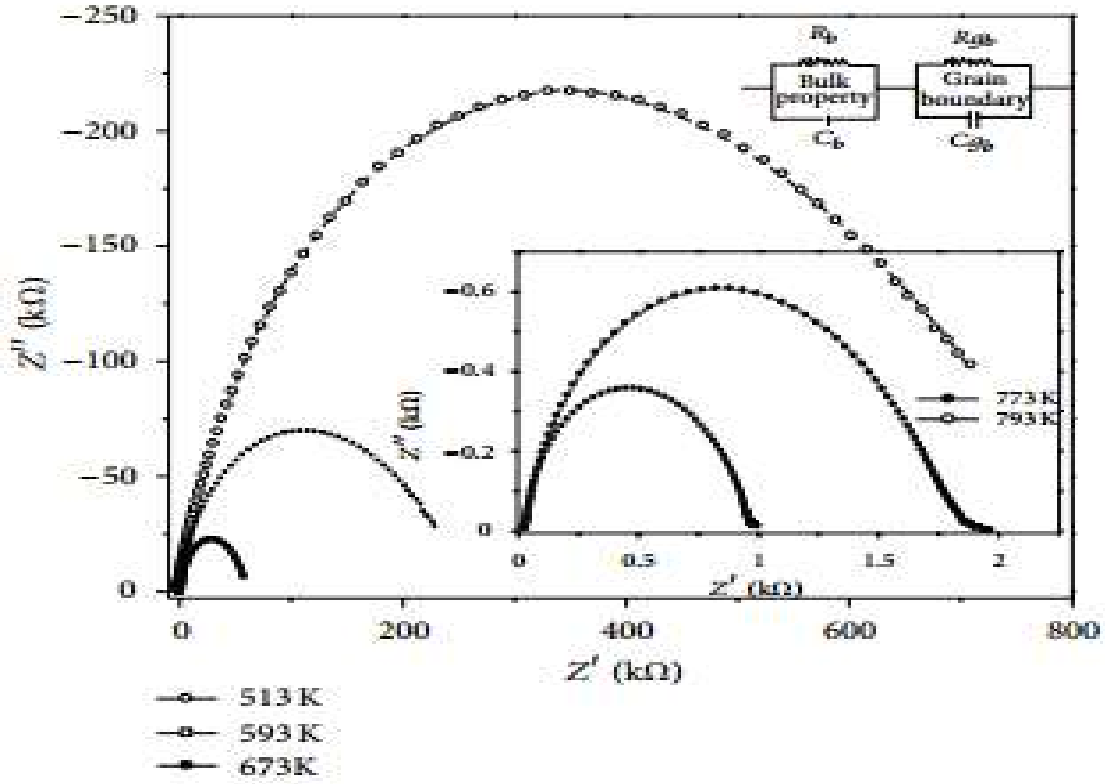

Figure 4.7: Nyquist plot of PbTiO3 (PT) material at five different temperatures. Figure in the inset shows the equivalent electrical circuit.

3.4. Complex Impedance Study.

Figure 7 shows the complex impedance spectrum of the PT compound at five different temperatures. From the nature of these plots, it is evident that the change in temperature ensures a distinct effect on the impedance spectrum of the material. The appearance of low temperature single circular arcs is due to the bulk properties of the material, and appearance of double arcs at high temperatures (inset Figure 7) is due to the consequence of bulk and grain boundary contribution to the conduction. These arcs appear in distinct frequency ranges, one at a higher frequency followed by another lower frequency arc. This feature is almost similar at different temperatures, also with a difference in radii of curvature of the arcs, which reduces with rise in temperature. The pattern in the impedance spectrum is a representative of the electrical processes taking place in the material which can be expressed as an equivalent electrical circuit comprising a parallel combination of resistive and capacitive elements. The presence of two arcs accordingly can be thought of as resulting from cascading effect of parallel combination of resistive and capacitive elements arising due to the contribution of bulk property of the material and grain boundary effect. The high frequency is attributed to the bulk property of the material (parallel combination of bulk resistance and bulk capacitance), and low frequency is due to the grain boundary effects in the material (parallel combination of grain boundary resistance and capacitance).

The electrical processes taking place within the material have been modeled on for a polycrystalline system and are shown in terms of the equivalent electrical circuit in the Figure 7 (inset). Figure 8 shows the variation Z'' with frequency at different temperatures. The average peak position regularly shifts towards higher frequency as the temperature increases. This insures the temperature dependent relaxation process in the sample. Furthermore, as evident from the plots, as the temperature increases, the magnitude $Z''$of decreases, the effect being more pronounced at the peak position. The shift of the peak towards higher frequency in raising the temperature is possibly due to the reduction in the bulk resistivity. The asymmetric peaks suggest the presence of electrical processes in the material with spread of relaxation time. The relaxation species may possibly be electrons or immobile species at lower temperature and defects at higher temperature that may be responsible for electrical conduction in the material.

Effectively large values of Z'' and Z'' at low frequencies or temperatures indicate a predominant effect of the polarizations which consists of large ε values of PTs. The intercepts of the two semicircles are used to calculate the bulk resistance (R_b) and grain boundary resistance (R_{gb}) while the corresponding frequency values evaluated from the apex of the semicircles have been used to calculate the bulk and grain boundary capacitance (C_b) using the relation, for a parallel combination of R and C

$$\omega_{\max} C_b R_b = 1 \qquad \text{or} \qquad \omega_{\max} C_{gb} R_{gb} = 1.$$

As temperature increases, both the grain resistance (R_g) and grain boundary resistance (R_{gb}) are found to decrease with rise in temperature indicated by a shift in the radius of the arcs towards left side on the real (Z') axis with increase in temperature. This provides convincing evidence that the electrical properties of PT are dependent on microstructure as well as temperature. A single nondegenarate process involves a single nondegenerate relaxation time for a given set of (R_b) and (C_b) at a temperature

$$\tau = C_b R_b = \frac{1}{\omega}.$$

The value of τ determined at selected temperatures in the region of measuring temperature using the values of (R_b)) and (C_b) in (9) is listed in Table 3. The τ -value is found to be decreasing linearly on increasing value of the temperature ($\sim$ above 600 K) suggesting a typical semiconductor behavior. The variation of τ with temperature (Figure 9) implies that the relaxation process is temperature dependent. The activation energy E_a evaluated from the slope of the curve by the relation

$$\tau = \tau_0 e^{-E_a/kT},$$

Where τ_0 is preexponential factor, E_a activation energy, k the Boltzmann constant and T the absolute temperature, is found to be 0.43 eV below 600 K and 2.1 eV above 600 K.

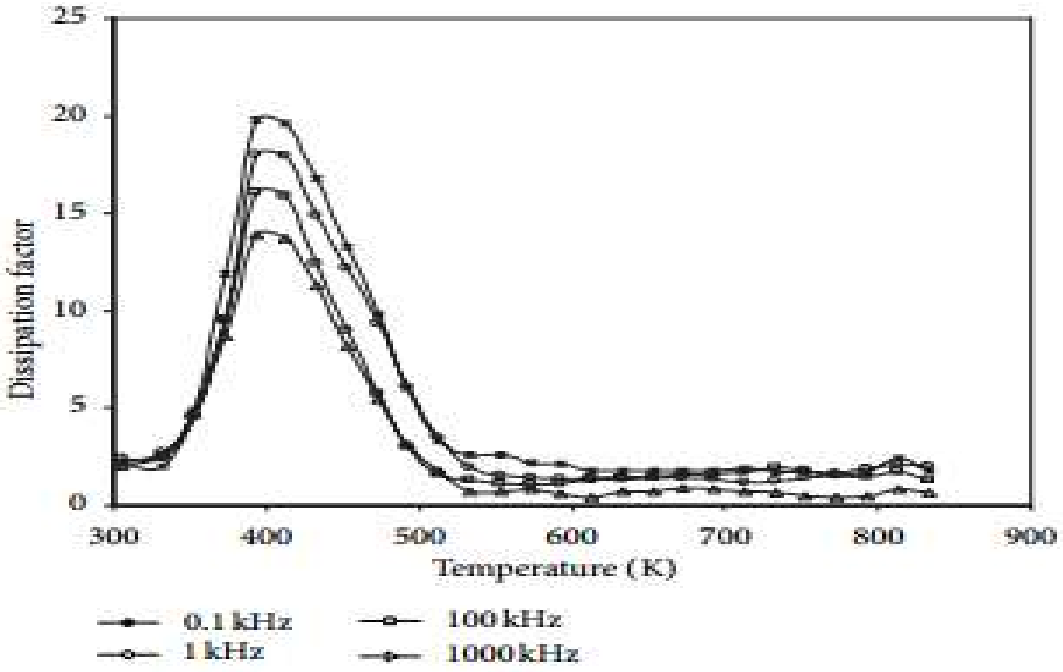

Figure 4.8: Temperature dependence of dissipation factor of PbTiO3 at different frequencies.

Table 3: Relaxation time calculated from impedance data for PbTiO3.

Temperature (°C)	R_g (Ω)	C_g (nF)	τ (s)
240	8.37×10^5	0.213	1.41×10^{-1}
320	2.47×10^5	0.202	3.42×10^{-2}
400	4.51×10^4	0.223	1.10×10^{-2}
440	9.87×10^3	0.204	5.92×10^{-3}
480	2.87×10^3	0.248	2.40×10^{-3}
500	2.00×10^3	0.316	1.53×10^{-3}
520	9.90×10^2	0.808	6.78×10^{-4}
540	6.44×10^2	0.554	2.46×10^{-4}

Another key feature is the texture of Pt. The idea behind that is that the texture of Pt assists the nucleation of the PT. The nucle-ation of PT and its growth behaviour is well described elsewhere [22]. During this work, the Ti thin film as well as the Pt layer was evaporated by e-beam evaporation in a BAK chamber supplied by Unaxis. The wafers were not heated during this process and the thin films therefore had an amorphous structure. To improve the crystallinity of Pt the wafers were tempered after manufac-turing with different temperatures. Tempering was performed in an inotherm high temperature oven for 30 min at a pressure of less than 0.1 Pa.

After tempering the above-described, GFS process was used to deposit PT. Fig. 3 shows a scheme of the setup in the chamber.

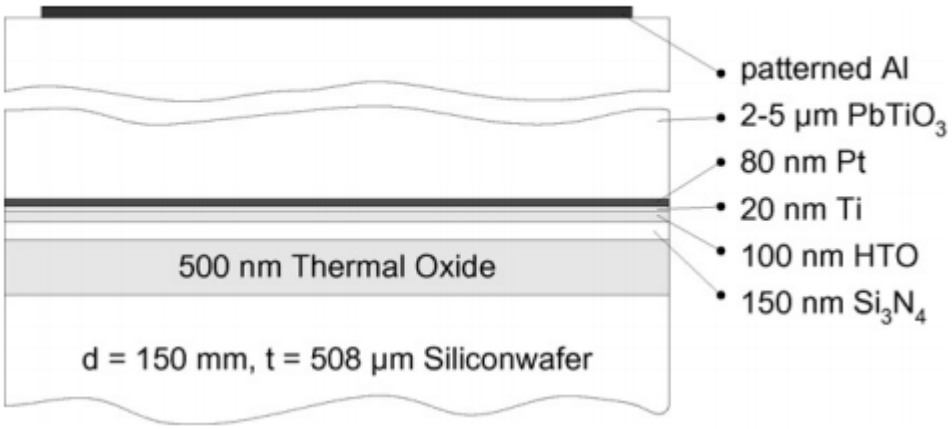

Fig. 4.9. Stack of the thin films in cross section.

The temperature of the chuck is measured during the sputtering by a thermocouple. Thin film processing of PT is very temperature sensitive. To be sure that the measured temperature of the chuck does not deviate too much from the real surface temperature of the substrate the setup is calibrated with melting probes of indium respectively tin. Fig. 4 shows the temperatures, measured at the chuck, to those moments when the probes are molten and the theoretical melting points of indium respectively tin.

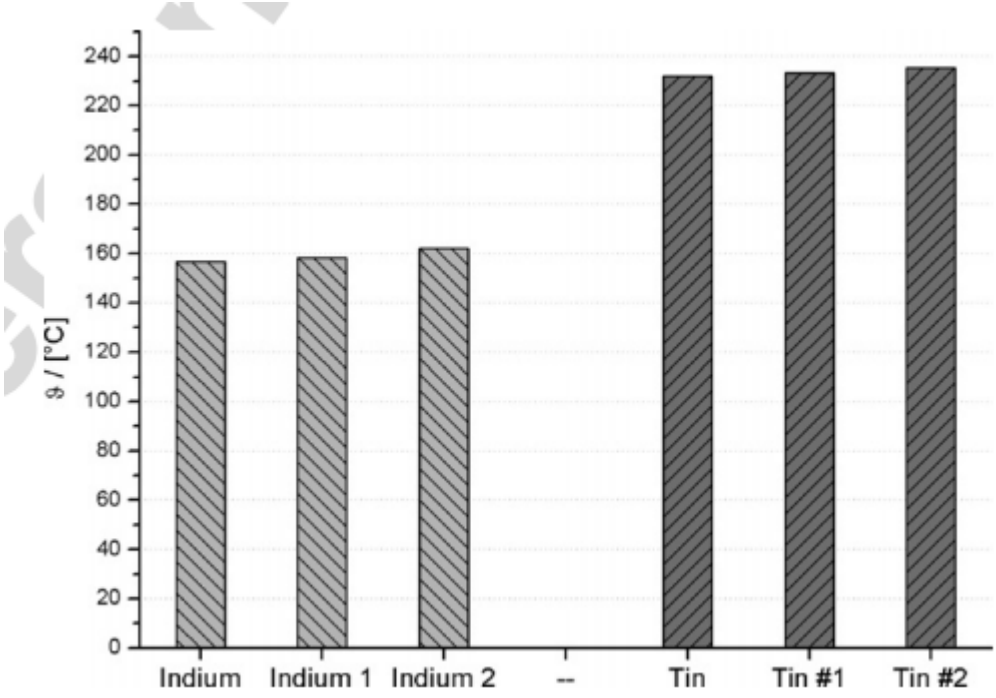

Fig. 4.10. Theoretical and measured melting points of indium and Tin.

CHAPTER 5: SUMMARY AND CONCLUSIONS

Based on the review that has been done in this work, the following conclusions and recommendations have been made. The conventional method of synthesizing PbTiO3 relies on the solid-state reaction between TiO2 and PbCO3 at high temperature. The conventional solid-state reaction has a tendency to produce a coarse PbTiO3 powder with compositional inhomogeneity and a degree of particle agglomeration if the processing parameters are not carefully optimized. Therefore, many chemistry-based processing routes, including co-precipitation, sol-gel synthesis, hydrothermal, and citrate routes, have been devised for the preparation of an ultrafine, sintering-reactive PbTiO3 powder. However, almost all these chemistry routes require calcination of the precursors at an elevated temperature to develop the desired PbTiO3 phase. Furthermore, most of these chemistry-based processing routes require high purity inorganic or organometallic chemicals as the starting materials, which are many times more expensive than the widely available oxides and carbonates. It has been observed that the synthesis of a mechanically robust, high density, monolithic ceramic pure PbTiO3 is not simple. Problems typically encountered include loss of lead (Pb) due to the volatility of PbO at elevated temperatures, porosity, and microcracking, in extreme cases leading to spontaneous fracture. The main hurdle in the PT fabrication is the synthesis of a single phase with required perovskite structure. The primary difficulty is due to the volatility of PbO at elevated temperatures. The PbTiO3 structure can only tolerate minor loss of lead (Pb), higher levels of which effectively promote second phase formation and the degradation of piezoelectric properties. An example is the formation of a PT phase with the pyrochlore structure observed during a coprecipitation synthesis experiment. A more common occurrence is the formation of a two-phase mixture with TiO2. The volatilization of PbO is known to increase markedly at temperatures above 800∘C though the critical temperature is debated. Kim et al. have observed that a PbO-rich PT in liquid phase is formed above 838°C, Alguero et al. found that at 650°C an excess of 20% PbO was required because of Pb-loss during thermal treatments of sol-gel prepared Lamodified PT thin films, whereas Ananta and Thomas found that Pb volatility in PMN-PT could be minimized by careful sintering up to 1250°C. What is clear is that the loss of lead depends on particle size of constituent oxides, processing conditions, and chemical stability. The degree of Pb incorporation into the presintered crystal structure affects the volatility enormously.

Many groups report that loss of lead (Pb) may be minimized by sintering compacted powders in a surrounding lead-based powder or a PbO vapor atmosphere although this may lead to a Pb gradient in the final sintered product. The problem of porosity has largely been addressed through particle size control of the starting powder. A careful and systematic study optimization of the synthesis parameters provides an alternative means of minimizing the problem of cracking, porosity, and Pb volatility. Careful sintering at lower temperatures may restrict grain growth and on cooling internal strains are reduced. In addition, sintering at low temperatures, the problem of volatility of lead is minimized. It has been shown that homogenous powders with a fine grain size can be produced by the ceramic process on the optimization of synthesis parameters. The electrical properties result from the different contributions made from various components and processes present in the material, and complex impedance spectroscopy has been commonly used to evaluate and separate the contribution of the overall electrical properties in the frequency domain due to electrode reactions at the electrode/sample interface and migration of ions through the grains and across the grain boundaries in a polycrystalline material. In view of this, we report our studies on electrical properties of PT samples using complex impedance spectroscopy technique. The frequency dependent properties of a material can be described via the complex permittivity (E), complex impedance (Z∗), and dielectric loss or dissipation factor (tan$). The peak of the semicircle in the complex plane plot enables us to evaluate the relaxation frequency (fmax) of the bulk material in accordance with the relation

$$\begin{aligned} \omega\tau &= 1, \\ (2\pi f)\,(R_b C_b) &= 1, \\ f &= \frac{1}{2\pi R_b C_b}, \end{aligned} \qquad (6)$$

Where Rb and Cb are the bulk resistance and capacitance, and f is the relaxation frequency. Relaxation frequency and relaxation time (t) depend on the intrinsic properties of the material and not on the sample geometrical factors. The term intrinsic properties of the material referred to the properties attributed to structure/microstructure (i.e., grain interior or bulk, grain boundary, etc.). These properties govern the distribution of resistive and capacitive components in the

material on which the relaxation time ultimately depends. In short, here we have made an attempt to optimize the synthesis parameters and further study the structural, microstructural, and electrical properties of the PT compound. The sintering behavior of the powders at various temperatures has been investigated using X-ray diffraction (XRD) patterns and scanning electron microscopy. The electrical behavior (complex impedance, complex permittivity, etc.) has been studied by complex impedance spectroscopy. The temperature and frequency variation of the electrical properties has also been investigated. The giant open circuit voltage (1700 V) has been observed for ITO/PLZT/Pt structure. It recommended to prepare and characterize the PT on different substrates, and with different other metal electrodes. The PT thin films were deposited by high rate gas flow sput-tering on silicon substrates using Pt bottom electrodes. The substrate were exposed to mid-frequency bias voltage and heated up to 600 $^{\circ}$C. Deposition rates of up to 120 nm/min were observed.

The XRD measurements showed clearly crystalline traces of PT without any post annealing. Furthermore it is on the one hand rather easy to create crystalline Pt thin films, but on the other hand it is enormously helpful to have already a crystalline bottom electrode for the nucleation and growth of PT. It could be observed that even the (1 1 1) texture of Pt is partial transferred to PT. The grain size of PT was estimated to 60 ± 20 nm. Only if the stoichiometry of the PT over the whole thin film at each point is equal to the empirical formula $PbTiO_3$, would it be possible for the whole material consists of 100% Perovskite. This is a rather theoretical case, but it is sine qua non to tune the stoichiometry as close as possible to the empirical formula. This is coarse done by modifying the ratio of the two target surfaces, but the stoichiometry is a function of many parameters. For fine tuning the stoichiometry of the thin films, it is important to adjust the chuck temperature with an accuracy of about 1 K and to keep it stable during processing.

References

Liu Y, Wang S, Chen Z and Xiao L (2016). Applications of ferroelectrics in photovoltaic applications, Science China Materials, 59, 851- 866.

Butler KT, Frost JM and Walsh A (2014). Ferroelectric materials for solar energy conversion: photoferroics revisited, Energy & Environmental Science, 8, 838-848.

Chen G, Zhang Y, Zhang Q, Lu Y and He Y (2020). Superior ferroelectric properties in Femodified (Pb,La) (Zr,Ti) O3 thin film by improving the remnant polarization and reducing the band gap, Ceramics International, 46, 15061-15065.

Zhang J, Su X, Shen M, Dai Z, Zhang L, He X, Cheng W, Cao M and Zou G (2013). Enlarging photovoltaic effect: combination of classic photoelectric and ferroelectric photovoltaic effects, scientific reports, 3, 2109.

Tiwari B, Babu T and Choudhary RNP (2020). Dielectric, impedance and modulus spectroscopy of Pb(Zr0.52-xCexTi0.48)O3 (x = 0.00, 0.10) ferroelectric ceramics, Physica Scripta, 95, 115806.

Yunxia Zhou, Jun Zhu, Xingpeng Liu and Zhipeng Wu (2017). Photovoltaic effect of ferroelectric Pb(Zr0.52,Ti0.48)O3 deposited on SrTiO3 buffered n-GaAs by laser molecular beam epitaxy, Functional Materials Letters, 10, 1750036.

Fengang Zheng, Yu Xin, Wen Huang, Jinxing Zhang, Xiaofeng Wang, Mingrong Shen, Wen Dong, Liang Fang, Yongbin Bai, Xiaoqing Shen and Jianhua Hao (2014). Above 1% efficiency of a ferroelectric solar cell based on the Pb(Zr,Ti)O3 film, Journal of Materials Chemistry A, 2, 1363-1368.

Zheng F, Zhang P, Wang X, Huang W, Zhang J, Shen M, Dong W, Fang L, Bai Y, Shen X, Sun H, and Jianhua Hao (2014). Photovoltaic enhancement due to surface-plasmon assisted visible-light absorption at the inartificial surface of lead zirconate–titanate film, Nanoscale, 6, 2915.

Yarmarkin V, Gol'tsman B, Kazanin M and Lemanov V (2000). Barrier photovoltaic effects in PZT ferroelectric thin films, Phys. Solid State, 42, 522–527.

Ichiki M, Maeda R, Morikawa Y, Mabune Y, Nakada T and Nonaka K (2004). Photovoltaic effect of lead lanthanum zirconate titanate in a layered film structure design, Appl. Phys. Lett., 2004, 84, 395–397.

Yao K, Gan BK, Chen M and Shannigrahi S (2005). Large photo-induced voltage in a ferroelectric thin film with in-plane polarization, Appl. Phys. Lett., 87, 212906.

Qin M, Yao K, Liang YC and Gan BK (2007). Stability of photovoltage and trap of lightinduced charges in ferroelectric WO3-doped (Pb0.97La0.03)(Zr0.52Ti0.48)O3 thin films, Appl. Phys. Lett., 2007, 91, 092904.

Qin M, Yao K and Liang YC (2008). High efficient photovoltaics in nanoscaled ferroelectric thin films, Appl. Phys. Lett., 93, 122904.

Zheng F, Xu J, Fang L, Shen M and Wu X (2008). Influence of work-function of top electrodes on the photovoltaic characteristics of Pb0.95La0.05Zr0.54Ti0.46O3 thin film capacitors, Appl. Phys. Lett., 93, 172101.

Cao D, Wang C, ZhengF, Dong W, Fang L and Shen M (2012). Nano Lett., HighEfficiency Ferroelectric-Film Solar Cells with an n-type Cu2O Cathode Buffer Layer, 12, 2803–2809.

Chen B, Zuo Z, Liu Y, Zhan QF, Xie Y, Yang H, Dai G, Li Z, Xu G and Li RW (2012). Tunable photovoltaic effects in transparent Pb(Zr0.53,Ti0.47)O3 capacitors, Appl. Phys. Lett., 100, 173903.

Ming Wu, Wei Li, Junning Li, Shaolan Wang, Yaqi Li, Biaolin Peng, Haitao Huang, and Xiaojie Lou (2017). Fatigue mechanism verified using photovoltaic properties of Pb(Zr0.52Ti0.48)O3 thin films, Appl. Phys. Lett. 110, 133903.

Yang Song, Lingwei Li, Yuanqing Chen, Fengzhu Li, Wenwen Qu, Huimin Wu, Aditya S. Yerramilli, Alford TL, and Haiwu Zheng (2018). Fabrication of PZT/CuO composite films and their photovoltaic Properties, Journal of Sol-Gel Science and Technology, 87, 285– 291.

Amador P´erez-Tomas, Haibing Xie, Zaiwei Wang, Hui-Seon Kim, Ian Shirley, SilverHamill Turren-Cruz, Anna Morales-Melgares, Benedicte Saliba, David Tanenbaum, Michael Saliba, Shaik Mohammed Zakeeruddin, Michael Gratzel, Anders Hagfeldt and Monica Lira-Cantu

(2018). PbZrTiO3 ferroelectric oxide as an electron extraction material for stable halide perovskite solar cells, Sustainable Energy Fuels, **3**, 382-389.

André Marino Gonçalves & José Antonio Eiras (2019). Time dependence of different contributions for the photovoltaic effect in ferroelectric PZT thin films with asymmetric electrodes, Ferroelectrics, 545:1, 22-32.

Anoop G, Juhee Seo, Chang Jo Han, Hyeon Jun Lee, Gil Woong Kim, Sung Su Lee, Eun Young Park, and Ji Young Jo (2015). Ultrathin platinum interfacial layer assistedphotovoltaic response of transparent Pb(Zr,Ti)O3 thin film capacitors, Solar Energy, 111, 118–124.

Harshan VN, Kotru S (2012). Influence of work-function of top electrodes on the photovoltaic characteristics of Pb0.95La0.05Zr0.54Ti0.46O3 thin film capacitors. Appl. Phys. Lett. 100, 173901.

G. Lilienkamp, C. Koziol, T. Schmidt, E. Bauer, X-Ray Microscopy and Spectromicroscopy, Springer-Verlag, Berlin, 1998.

V. A. Chaudhari and G. K. Bichile, Synthesis, Structural, and Electrical Properties of Pure PbTiO3 Ferroelectric Ceramics